CATION AND ANION ADSORPTION BEHAVIOR

ON

OXIDE SURFACES

By

Cristian Pablo Schulthess

A dissertation submitted to the Faculty of the University of Delaware in partial fulfillment of the requirements for the degree of Doctor of Philosophy in Plant Science

December, 1987

CATION AND ANION ADSORPTION BEHAVIOR

ON

OXIDE SURFACES

By

Cristian Pablo Schulthess

Approved: Donald L. Sparks

Donald Lewis Sparks, Ph.D.
Professor in charge of dissertation on behalf of the Advisory Committee

Approved: A. L. Morehart

A. Morehart, Ph.D.
Chairman of the Department of Plant Science

Approved: Richard B Murray

Richard B. Murray, Ph.D.
Associate Provost for Graduate Studies

EPIGRAPH

For the validity of their conceptual and experimental methods, most scientists depend on assurances from reputable predecessors in their field. The latter individuals in turn have usually adopted the procedures from some comparable person who preceded them. If the forerunners in the use of a technique have not recognized its limitations or have obscured them, a tradition of analysis may develop that generates pervasive misinformation in the scientific literature.

Klotz, I.M. 1982. Science 217:1247–1249.

ACKNOWLEDGEMENTS

I am deeply indebted to Dr. Donald L. Sparks for his constant encouragement and support. Immense appreciation is also extended to the committee members, Dr. J. Thomas Sims, Dr. Steven K. Dentel, Dr. Ronald J. Gibbs, and Dr. Allen L. Morehart for their suggestions and constructive criticisms.

I gratefully thank Jerry Hendricks (the lab's Headman), Richard Ogwada, Ted Carski, Mark Noll, Maria Sadusky, Chip Toner IV, Pengchu Zhang, and Mat Eick for their comradery. This is also acknowledged for Mark Seyfried, Asher Bar Tal, and Nanak Pasricha. The faith and support from my parents and friends has always been appreciated, thank-you for your prayers.

This research was financially supported through a University Graduate Research Fellowship, and the Hatch funding provided by the College of Agricultural Sciences (Hatch Act of 1887).

DEDICATION

... to Jennifer Ellen ...

TABLE of CONTENTS

LIST of TABLES

LIST of FIGURES

ABSTRACT

The chemical and physical behavior of solid particles in an aqueous medium are affected by the interactions present at the solid-aqueous interface. Chemical reactions (e.g., cation and anion adsorption) and physical observations (e.g., electrokinetics) elucidate the nature of the interface; however, these experiments generally result in contradicting data. This research found that the inconsistencies are due to an overlapping of a pH-dependent solubility phenomena on the solid-aqueous phase interactions. This is particularly significant in potentiometric titration analyses that measure the proton adsorption isotherms with respect to pH.

This dissertation critically challenges current theories on the pH-dependent behavior of oxides with respect to cation exchange capacity, anion exchange capacity, potential determining ions, inert electrolytes, electrokinetics, and surface charge models. Methodologies and models commonly used in solid-aqueous interface research are critically reviewed based on Al and Si oxide studies, and a modification of the potentiometric titration procedure was developed, called the *backtitration technique*. The backtitration technique results in accurate proton

adsorption isotherms due to the adjustments made for the variable solubility of the solid phase. This in turn allows development of proton adsorption models with an entirely new set of data. Specifically, an Al oxide is easily modeled with pH and salt-dependent reactions competing with salt-dependent reactions. The maximum number of sites is readily determined from the data without any further mathematical manipulations. Furthermore, the proton isotherms are stoichiometrically related to the cation and anion isotherm behavior. This allows predictions on cation and anion adsorption behavior based on the proton adsorption isotherm model.

It is strongly suggested that the Boltzmann distribution term in models using intrinsic equilibrium constants is merely tracking the solubility behavior of the solid phase. It is hypothesized that the oxide surface is neutral at all times; the charged behavior observed in electrokinetic studies is induced by the applied electric field that shears the aqueous counterions in one direction and the oxide surface in the opposite direction. In the absence of an applied electric field the oxide particles are neutral, and the only surface reactions present are ion exchange reactions.

CHAPTER 1

INTRODUCTION

[1.1] EARLY HISTORY of ION EXCHANGE STUDIES

Our current understanding of chemistry is due mostly to two chemical revolutions. The first occurred in 1770–1800 (also called Lavoisier's revolution) with the introduction of the concept of elements as the most basic fundamental substances, and with the final end to Aristotle's (384–322 B.C.) concept of four elements: earth, water, air, and fire (Ihde, 1984). The second revolution is dated at 1860 with the discovery of cesium; however, the era is noted for the eventual establishment of a sound system of classification of the elements made possible after Cannizzaro proved methods for determining correct atomic weights in 1858 (Ihde, 1984). The history of solid phase chemistry should begin with Scheele, known best for his 1777 "Treatise on Air and Fire." Considered the "supreme

experimental chemist of his century" (Chalmers, 1949), he discovered the capacity of coals to absorb gases in 1773 (Urdang, 1942); however, credit usually goes to Fontane who demonstrated the phenomena in 1777 (Nordenskiöld, 1892). In 1785, Lowitz accidentally discovered that powdered charcoal effectively removed visible impurities from his tartaric acid solution (Figurovsky, 1973). He subsequently recommended that the adsorbing charcoal be used as a purifying agent for vodka, sugar syrup, and drinking water (Figurovsky, 1973).

The term *adsorption* for ions that are chemically bound may have been coined by Kayser (1881), and should not be confused with the much older term *absorption* for ions that are physically bound to the surface. McBain (1909) coined the term *sorption* since it was often difficult to distinguish between the absorption and adsorption phenomena.

In soil chemistry, Thompson (1850) and Way (1850, 1852) were perhaps the first to quantitatively study cation exchange. They found that as a solution of $(NH_4)_2SO_4$ was added to a column of soil, $CaSO_4$ was leached. Way's conclusions were so revolutionary that he is now honored as the "Father of Soil Chemistry" (Thomas, 1977). Johnson (1859) corrected some of Way's conclusions, particularly that adsorption is reversible, and coined the term *exchange of bases* for Way's observations.

In colloid physical chemistry, Helmholtz (1879) introduced the concept of a double-layer of electricity at the interface of the surface and the liquid. These theories were based on electrokinetic studies of particles; viz., studies of the movement of these particles in the presence of an applied electric field. Briefly, the inner layer includes the charged particles that travel towards one of the electrodes, while the outer layer includes the counterions that travel in the opposite direction. Gouy (1910) and Chapman (1913) further advanced this concept to the diffuse double-layer (DDL) theory of particles in an aqueous medium.

By the 1900's, studies on the effect of soil acidity were conducted with phenolphthalein indicators. Böttger (1897) introduced electrometric methods for determining the H^+ ion concentration. Sørensen (1909) introduced colorimetric methods for determining the H^+ ion concentration, and coined the term *pH* (or Sørensen value) to refer to the negative logarithmic value of the H^+ ion concentration: $pH = -\log[H^+]$, or $[H^+] = 10^{-p}$. The letter *p* is the initial letter of the words *Potenz, puissance,* and *power,* and was called the "hydrogen ion exponent" by Sørensen (Bates, 1974). The pH term was not immediately used in general chemistry; however, it was used extensively in agricultural science and physiology (E. Fisher, 1921a). G. Fisher may have been the first to potentiometrically measure the pH of soil suspensions in 1914 (E. Fisher, 1921b). This type of research soon led to the concept of clays acting as amphoteric surfaces (Arrhenius, 1922; Mattson, 1931); viz., surfaces with both acidic and

basic characteristics. Early studies on the pH dependence of adsorption were made by Mattson (1931) and Kurbatov et al. (1951), and this is still an important issue in soil and colloidal chemistry.

To discuss the evolution of all the theories and experimental procedures that have developed since 1800, and particularly since 1900, is beyond the scope of this chapter. However, current theories and methodologies that are related to the topics of this dissertation are discussed in the introductory section of each of the chapters.

[1.2] SOLID-AQUEOUS PHASE CHEMISTRY

Soil, from a chemical point of view, functions primarily (i) as a reservoir and buffering zone for nutrient exchange essential for plant growth, (ii) as a retainer for organic chemicals, (iii) as an intermediate phase with respect to groundwater quality, and (iv) as an interacting medium with both liquid and vapor phases. Elements or compounds which are held by the soil under one set of conditions, may be released by the soil under another set of conditions; changes in the soil environment are often plant-induced. An understanding of these reactions leads to better farming practices and environmental quality through the introduction of man-induced changes in the soil environment.

The effect of soil pH on the fate of essential nutrients, and subsequently on the crop yield and groundwater quality, has been recognized as the most important environmental parameter as well as the easiest to change by plant-induced root secretions or farming practices. Soil pH also plays a major role in soil stability and weathering of minerals.

Interest in the chemical interactions and pH dependence of the solid phase with the aqueous phase is shared by several research fields. These include: environmental engineering in water treatment and purification, chemical engineering in enhancing stability of suspended particles, marine studies in particle coagulation and rate of settling, and microbiology in nutrient uptake. Hayes et al. (1987) also include to this list: electrical engineering in ion-sensitive field effect transistors; catalysis in doping of oxide supports; material science in corrosion control; and geochemistry in ore deposition, metal extraction, and weathering. It is interesting to note differences in research objectives such that aquatic and colloid research considers a *floc* to be stable if it remains dispersed, whereas soil science research considers a *soil* to be stable if it does not disperse. However, the conclusions are shared due to the common interest in the chemistry of the solid-aqueous phase of particles.

There are various experiments that are often applied to colloids and soils. These include: (i) potentiometric (acid/base) titration analysis for determining

proton adsorption isotherms, maximum number of surface sites, and surface charge; (ii) cation exchange capacity (CEC) and anion exchange capacity (AEC) studies for determining ion adsorption isotherms, maximum number of surface sites, and surface charge; (iii) electrokinetics for surface charge studies only; and (iv) coagulation and rate of settling studies for determining particle size and stability. Surface charge has traditionally been considered responsible for nearly all solid/aqueous phase physicochemical phenomena. The first two analyses mentioned above measure surface charge indirectly. The third analysis measures surface charge directly (more specifically, at the plane of shear), and the fourth set of analyses are affected by surface charge. However, all of these experiments often disagree in physical interpretation, magnitude, and chemical mechanisms or reactions involved in surface charge phenomenon. Since surface charge is the cornerstone to a long list of soil and colloidal behavior, it is essential to formulate mathematical predictions with corresponding physical illustrations. The research emphasis must be to pursue models that are consistent with data from a variety of independent experiments.

The objectives of this research were: (i) to evaluate potentiometric titration methods of solid suspensions, and critically assess the validity of the data; (ii) to compare the most accurate potentiometric titration data with CEC-AEC data, and critically assess the differences and similarities of these two methods; and (iii) to compare the potentiometric titration data with electrokinetic data, and

critically assess the differences or similarities of these two methods. Also, (iv) mathematical adsorption models and surface physical interpretations were pursued to help elucidate the nature of the solid-aqueous phase physical chemistry of oxide particles.

CHAPTER 2

BACKTITRATION TECHNIQUE
for PROTON ISOTHERM MODELING of OXIDE SURFACES

[2.1] INTRODUCTION

Before characterizing and modeling the surface charge behavior of a soil or colloidal system, one must decide which method to use, what terminology to adopt, and how the model will be used to interpret the data. Some of the methods available involve electrokinetics, cation-anion exchange, and potentiometric titration curves.

Unlike electrokinetics, which involves the entire colloid, the cation-anion exchange and potentiometric titration methods measure surface sorption behavior. These data are then interpreted in terms of surface charge, or permanent charge, according to the sorption model used. Veitch (1904) made an early attempt to

compare the accuracy and practicality of two methods to determine soil acidity: the NaCl method (cation exchange) and the lime-water method (titrimetric), recommending the latter. Interest in titrating soils soon led to interpretive complications. Potentiometric titration curves of soils yield no definite breaks to indicate end points, as is usually expected of weak acids. Bradfield (1923, 1924) claimed that the error was due to methodology. He obtained "definite breaks" by adding the soil (weak acid) to the alkali solution (strong base) as is usual for chemical analyses. Mattson (1931) called the pH of exchange neutrality (EN) to be the pH where anion adsorption equals cation adsorption. He made very extensive studies on the relationship between pH and ion exchange, and treated the soil surfaces as behaving amphoterically. Grahame (1947) gave an excellent review on electrical double-layer theory and helped set the stage for future modeling of surface charge. Schofield (1949) challenged the "old" titration methods and suggested using a cation-anion exchange method with acid NH_4Cl. His work, and that of others who followed, greatly influenced the field of soil science. It became acceptable to use ion exchange methods to determine surface charge (CEC vs. AEC), and potentiometric titrations were generally reserved for zero point of charge (ZPC) analyses only.

Various interpretations of potentiometric titration curves are still being presented. Westall and Hohl (1980) compared five electrostatic models of the oxide-solution interface and found them all to fit the potentiometric data rather

well. Lyklema (1968) observed that the surface charge vs. pH curves for all oxides are convex. Since this leads to high surface charge density, he postulated a potential and charge distribution inside the solid assuming an exponential decay of porosity, with large radii ions having low penetration depth. Parks and de Bruyn (1962) argued that the ZPC was at the pH of minimum solubility of the solid species.

Another challenge for soil and colloid chemists is the myriad of "zero point" vocabulary. Parker et al. (1979) insisted that terms like zero point of charge (ZPC), or isoelectric point (IEP) are too vague. They suggested terms like point of zero salt effect (PZSE) and point of zero net charge (PZNC). Sposito (1981) also suggested the term point of zero net proton charge (PZNPC). Bowden et al. (1977) used the terms isoelectric point of the solid (IEPS) and pristine point of zero charge (PPZC), and Hendershot (1978) worked with zero point of titration (ZPT). Furthermore, the abbreviations ZPC and PZC are used interchangeably.

Parks (1965) reviewed reported ZPC values for oxides using electrokinetics. There seems to be general agreement on the values reported with only a few exceptions. Additionally, Parks (1967) proposed using a weighted average of the component ZPC values of the soil matrix as an initial estimate of the soil's ZPC value. Parfitt (1980) observed that "isoelectric weathering" may also take place in that the ZPC approaches the soil pH with time.

This chapter is primarily concerned with determining why potentiometric titration curves yield surface charge vs. pH data. The assumptions and limitations of three "singular reference curve" methods commonly found in the literature will be discussed in detail. Finally, a "backtitration technique" will be presented to better describe the solid-solution interface, and it will be used to model the proton isotherm on an Al oxide surface. In evaluating methodologies it is advisable to work with simple systems so as to avoid possible secondary effects that might obscure "obvious" results. A γ-Al_2O_3 colloid was chosen for this study because of the great importance of Al oxides in soils, especially tropical soils. The theoretical discussion that follows is applicable to all potentiometric titrations.

[2.2] MATERIALS and METHODS

[2.2.1] Theoretical Considerations

The principle of electroneutrality must hold true for every point on all titration curves, i.e., the sum of all negative charges is equal to the sum of all positive charges

$$\sum \text{negative charges} = \sum \text{positive charges} . \qquad [2.1]$$

For example, the titration of an amphoteric oxide surface with $HClO_4$ or NaOH in the presence of $NaClO_4$ electrolyte solution, would result in

$$(OH^-) + (ClO_4^-) + \left\{ \begin{matrix} \text{negative} \\ \text{surface} \end{matrix} \right\} = (H^+) + (Na^+) + \left\{ \begin{matrix} \text{positive} \\ \text{surface} \end{matrix} \right\} \qquad [2.2]$$

or,

$$\sigma_o = \left\{ \begin{matrix} \text{positive} \\ \text{surface} \end{matrix} \right\} - \left\{ \begin{matrix} \text{negative} \\ \text{surface} \end{matrix} \right\} = (C_A - C_B) - (\mathrm{H^+} - \mathrm{OH^-}) \qquad [2.3]$$

where σ_o = surface charge,

$\left\{ \begin{matrix} \text{negative} \\ \text{surface} \end{matrix} \right\}$ = conc. of negative charges on the surface of the colloid,

$\left\{ \begin{matrix} \text{positive} \\ \text{surface} \end{matrix} \right\}$ = conc. of positive charges on the surface of the colloid,

$(\mathrm{H^+}) \quad = 10^{-\mathrm{pH}}$,

$(\mathrm{OH^-}) \; = 10^{\mathrm{pH}-\mathrm{pK_w}}$,

$(\mathrm{ClO_4^-}) = (\mathrm{NaClO_4})_{\text{added}} + (\mathrm{HClO_4})_{\text{added}}$,

$(\mathrm{Na^+}) \; = (\mathrm{NaClO_4})_{\text{added}} + (\mathrm{NaOH})_{\text{added}}$, and

$(\mathrm{ClO_4^-}) - (\mathrm{Na^+}) = (\mathrm{HClO_4})_{\text{added}} - (\mathrm{NaOH})_{\text{added}} = C_A - C_B$.

When the surface charge is neutral, the negative and positive charges are equal, $\left\{ \begin{matrix} \text{negative} \\ \text{surface} \end{matrix} \right\} = \left\{ \begin{matrix} \text{positive} \\ \text{surface} \end{matrix} \right\}$, and the surface is said to have zero charge. At the pH of ZPC, Eq. [2.3] simplifies to:

$$(C_A - C_B) - (\mathrm{H^+} - \mathrm{OH^-}) = 0 \; . \qquad [2.4]$$

The question one may ask is, how does one know at what pH value does Eq. [2.4] hold true? Gouy (1910) and Chapman (1913) derived an equation correlating the potential of a surface to the surface charge

$$|\sigma_o| = \left(\frac{2\mathrm{kT}\varepsilon n_o}{\pi} \right)^{\frac{1}{2}} \sinh \left(\frac{\mathrm{ze}\Psi_o}{2\mathrm{kT}} \right) \qquad [2.5]$$

where σ_o = surface charge, esu/cm^2; 1 esu/cm^2 = 1 g$^{1/2}$cm$^{-1/2}$s^{-1}

= 3.4607×10^{-12}mmol/cm^2;

Ψ_o = surface potential, statvolt; 1 statvolt = 300 volts;

n_o = electrolyte concentration, ions/cm^3;

ε = dielectric constant = 80 for H_2O at 293°K;

e = unit charge = 4.80×10^{-10} esu/ion;

z = valence of ion; and

kT = energy term = (1.38×10^{-16} ergs ion^{-1}deg^{-1}) × (abs. temp.) .

Using Nernst's (1889) equation the surface potential can be correlated to the concentration of potential determining ions (PDI) in solution:

$$\Psi_o = \frac{\mathrm{kT}}{\mathrm{ze}} \ln \frac{C}{C_o} \qquad [2.6]$$

where C = concentration of PDI, and

C_o = concentration of PDI when $\Psi_o = 0$.

The PDI for the experiments in this study are H^+ and OH^-. The Na^+ and ClO_4^- ions are assumed to be indifferent at the surface and not to act as PDI (Yopps and Fuerstenau, 1964). Thus, the adsorption of H^+ or OH^- onto the surface is assumed to control the charge of the surface studied. Substituting $C = (H^+)$ and $C_o = (H^+)_{ZPC}$, combining Eq. [2.5] with [2.6], and substituting $\frac{\ln(H^+)}{2} = 1.15\log(H^+) = -1.15\mathrm{pH}$ gives

$$|\sigma_o| = \left(\frac{2\mathrm{kT}\varepsilon n_o}{\pi}\right)^{\frac{1}{2}} \sinh\{1.15(\mathrm{pH_{ZPC}} - \mathrm{pH})\} . \qquad [2.7]$$

Combining Eq. [2.3] and [2.7] gives

$$\sigma_o = \left\{ \begin{matrix} \text{positive} \\ \text{surface} \end{matrix} \right\} - \left\{ \begin{matrix} \text{negative} \\ \text{surface} \end{matrix} \right\}$$
$$= (C_A - C_B) - (\mathrm{H}^+ - \mathrm{OH}^-)$$
$$= \pm \left(\frac{2\mathrm{kT}\varepsilon n_o}{\pi} \right)^{\frac{1}{2}} \sinh\{1.15(\mathrm{pH_{ZPC}} - \mathrm{pH})\} \; . \qquad [2.8]$$

If $\mathrm{pH} = \mathrm{pH_{ZPC}}$, then $\sigma_o = 0$ and $\left\{ \begin{matrix} \text{negative} \\ \text{surface} \end{matrix} \right\} = \left\{ \begin{matrix} \text{positive} \\ \text{surface} \end{matrix} \right\}$ for any ionic strength. If $\mathrm{pH} > \mathrm{pH_{ZPC}}$, then $\sigma_o < 0$ and $\left\{ \begin{matrix} \text{negative} \\ \text{surface} \end{matrix} \right\} > \left\{ \begin{matrix} \text{positive} \\ \text{surface} \end{matrix} \right\}$. Conversely, if $\mathrm{pH} < \mathrm{pH_{ZPC}}$, then $\sigma_o > 0$ and $\left\{ \begin{matrix} \text{negative} \\ \text{surface} \end{matrix} \right\} < \left\{ \begin{matrix} \text{positive} \\ \text{surface} \end{matrix} \right\}$. Furthermore, at a fixed pH value $> \mathrm{pH_{ZPC}}$, an increase in electrolyte concentration, n_o, will increase both $|\sigma_o|$ (making σ_o more negative) and C_B (more base is needed to attain the pH value desired). At a fixed pH value $< \mathrm{pH_{ZPC}}$, an increase in n_o will increase both $|\sigma_o|$ (making σ_o more positive) and C_A (more acid is needed to attain the pH value desired). Thus, if several charge curves (σ_o vs. pH) at various ionic strengths are superimposed, the pH value where the curves intersect is the ZPC.

The following methods below outline various ways in which Eq. [2.8] may be applied. The results and limitations of each method will be discussed later. The colloid studied was a γ-Al_2O_3 made by the Degussa Corp., of Teterboro, NJ, under the trade mark name of Aluminum Oxide-C. A stock suspension of 105 g L^{-1} was prepared with deionized water and allowed to equilibrate for several days before use. The concentration of the oxide suspension was checked by gravimetric analysis. The oxide had a BET surface area of 100 ± 15 m^2 g^{-1}, and the average primary particle size (dry) was 20 nm (supplied by the manufacturer).

Method I

The γ-Al_2O_3 titration data were applied to Eq. [2.3] to estimate the surface charge. Plotting surface charge vs. pH should yield three lines intersecting at the pH of ZPC.

Method II

An electrolyte solution, prepared by adding 10 mL of deionized water rather than 10 mL of the colloidal suspension, was also titrated by a simple acid-base titration method where the pH was recorded for each increment of 0.25 M acid or 0.25 M base that was added. This procedure was repeated for various ionic strengths and plotted as pH vs. mmol of acid (or base) added to the electrolyte solution. From each graph, the difference in mmol of acid (or base) added at a given pH value between the titration of the colloidal sample and the titration of the corresponding electrolyte solution was measured and plotted separately as surface charge vs. pH for each ionic strength. The pH value where these lines intersect each other is referred to as the ZPC.

Method III

Several samples were made with no acid or base additions. After these "zero addition" samples were equilibrated overnight and pH measured along with the other samples, they were centrifuged and filtered through 0.2 μm filter paper. The

[2.2.2] Experimental Procedures

A batch titration of the colloid was made using 125 mL polyethylene bottles containing 10 mL of the γ-Al_2O_3 suspension (105 g L^{-1}), and a predetermined amount of $NaClO_4$ for various initial ionic strength settings (e.g., 2 mL of 0.25 *M* $NaClO_4$ will yield I = 0.01 *M* in a 50 mL sample). To a row of approximately 20 samples, varying amounts of 0.25 *M* $HClO_4$ or 0.25 *M* NaOH solutions were added to vary the pH in each sample. For example: half a batch may contain 500, 400, 300, 250, 200, 150, 100, 75, 50, 25, and 10 μL of 0.25 *M* NaOH, and the other half may contain similar amounts of 0.25 *M* $HClO_4$. There was also at least one sample with no acid or base additions. The volume of acid or base additions were carefully monitored by the use of 2.000 mL micrometer syringes (distributed by Cole-Parmer Inst. Co., Chicago, IL) which deliver the desired solution in 0.002 mL increments. Each sample was then diluted to a final volume of 50 mL with deionized water.

Finally, after all the additions were made, the samples were tightly capped and shaken overnight on a reciprocating shaker at room temperature. After equilibrating, the suspension pH of each sample was measured and the pH data of the entire batch were plotted against mmol of acid (or base) added. The process was repeated for three ionic strengths (0.001, 0.01, and 0.1 *M*). Each run was repeated in parts to ensure reproducibility and detail of the resulting curves. The data and their resulting curves were used in methods I, II, and III which are outlined below. Each sample was saved and later treated according to method IV given below.

supernatant of these "zero addition" samples, which will be referred to as ZPT supernatant solutions, were used as the blank reference. This blank consists of the electrolyte solution in which all the samples were suspended in, plus all the species which are soluble under the particular pH condition of no acid or base addition. A 50 mL aliquot of this blank reference solution was titrated and the pH was recorded for each increment of 0.25 *M* acid or 0.25 *M* base that was added. The data were plotted as mmol of acid (or base) added vs. pH. For each ionic strength run the difference in mmol of acid (or base) added for the colloid titration and the blank reference titration at any given pH value was measured and plotted as surface charge vs. pH. The pH value where these lines intersect each other is referred to as the ZPC.

Method IV

After equilibrating overnight and measuring the pH of the suspensions, all the samples were individually centrifuged and filtered. Each of the supernatants was weighed, pH measured, and backtitrated with pH 7 as the end point. The backtitrations were done with an autotitrating system (Radiometer, Copenhagen, Denmark) using a constant titration rate of 0.5 or 0.05 mL min^{-1}, and 0.03 *M* $HClO_4$ as the titrant for the alkaline supernatants or 0.03 *M* NaOH as the titrant for the acidic supernatants. The volume of titrant added to the supernatants, V_{BT}, was the volume necessary to achieve a supernatant pH of 7.00. Since the

volume of the supernatant was never equal to the initial 50 mL due to losses in the separation and filtration process, the V_{BT} values were adjusted linearly with respect to the weight recovered. The difference between mmol of acid (or base) added and the solution alkalinity (or acidity) remaining yields the μmol m^{-2} of H^+ adsorbed or desorbed (Γ_{H^+,OH^-}):

$$\Gamma_{H^+,OH^-} = \left[(V_A C_A - V_B C_B) + (V_{BT_A} C_{BT_A} - V_{BT_B} C_{BT_B})\frac{50\rho}{W}\right] \times 10^3/\mathrm{Ag} \quad [2.9]$$

where subscript A = acid; B = base;

W = weight of supernatant backtitrated, g (max. weight = 50 g);

ρ = density of supernatant (assume ρ =1.00 g mL^{-1});

V = volume of acid or base added to the colloid suspension, mL;

C = concentration of titrant = 0.25 M;

V_{BT} = volume of acid or base added in backtitration, mL;

C_{BT} = concentration of backtitrant = 0.03 M;

$10^3\mu$mol = 1.0 mmol; and

Ag = (specific surface area)×(weight of colloid titrated)

= $(10^2 m^2 g^{-1})\times(1.05\ g)$.

Proton adsorption and hydroxyl desorption are experimentally indistinguishable. The Γ_{H^+,OH^-} values were plotted against the supernatant pH for each batch run and repeated for several ionic strengths. The surface charge and the amount of acid sorbed are not synonymous terms.

[2.3] RESULTS and DISCUSSION

[2.3.1] Singular Reference Curves (Methods I, II, and III)

Figure 2-1 shows the pH of the suspension vs. the mmol of acid or base added to the colloid. Solving Eq. [2.3] with the oxide titration data shown in Fig. 2-1, yields the surface charge vs. pH behavior shown in Fig. 2-2. This procedure assumes that the only reactions involved in the system are with the hydronium or hydroxyl ions either sorbing or desorbing from the oxide surface, and that no reactions exist in the aqueous bulk solution. The ZPC is at the intersection of the three ionic strength conditions as anticipated by Eq. [2.8]. The surface charge scale is shifted to set a value of zero charge at the intersection in Fig. 2-2.

Rather than solving Eq. [2.3] for each data point, the solution to the equation of electroneutrality may be done graphically. That is, if a reference solution without the colloid sample is titrated, then the surface charge would be

$$\sigma_o = (C_A - C_B)_{\text{sample}} - (\text{H}^+ - \text{OH}^-)_{\text{sample}}$$

$$- 0 = (C_A - C_B)_{\text{ref}} - (\text{H}^+ - \text{OH}^-)_{\text{ref}}$$

$$\sigma_o = (C_A - C_B)_{\text{sample}} - (C_A - C_B)_{\text{ref}} + (\text{H}^+ - \text{OH}^-)_{\text{ref}} - (\text{H}^+ - \text{OH}^-)_{\text{sample}} \qquad [2.10]$$

and if $(\text{H}^+ - \text{OH}^-)_{\text{ref}} = (\text{H}^+ - \text{OH}^-)_{\text{sample}}$, such as by subtracting the reference curve from the sample curve at a given pH value, then

$$\sigma_o = (C_A - C_B)_{\text{sample}} - (C_A - C_B)_{\text{ref}} = \Delta(C_A - C_B)\ . \qquad [2.11]$$

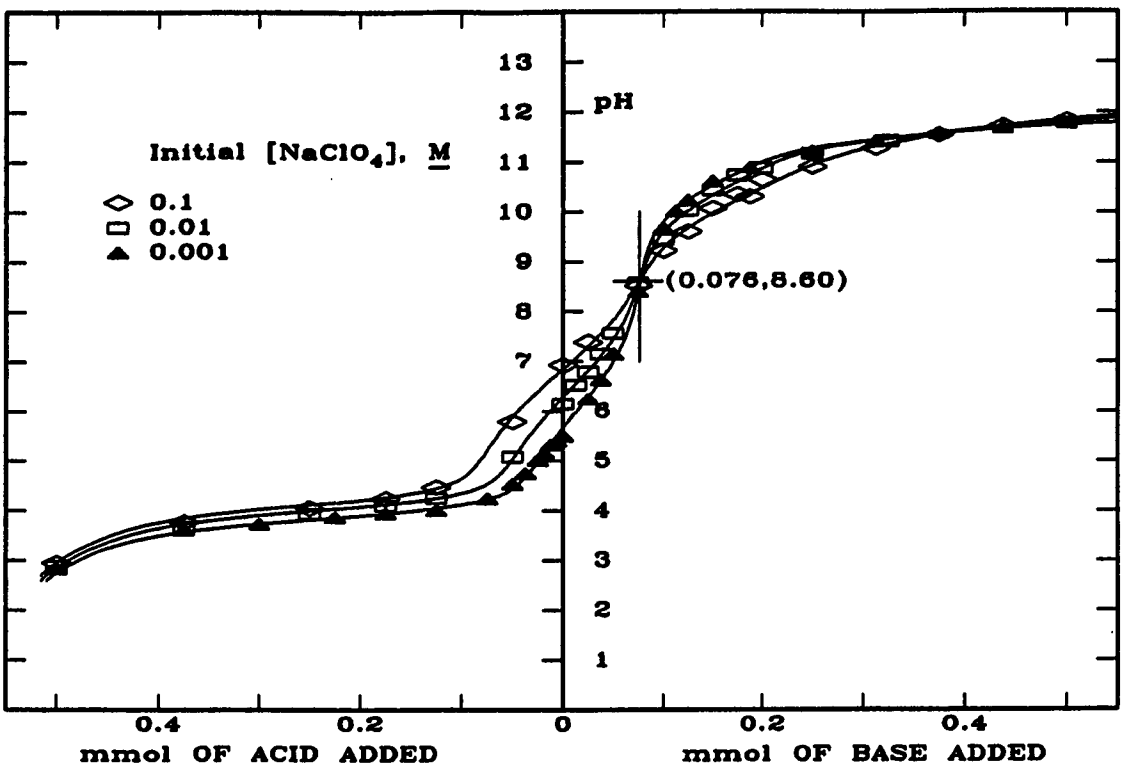

Fig. 2-1. Batch titration of γ-Al_2O_3 at various ionic strengths with $HClO_4$ and NaOH. [γ-Al_2O_3] = 1.05 g 50 mL^{-1}, total volume = 50 mL, pH of suspension after equilibrating overnight.

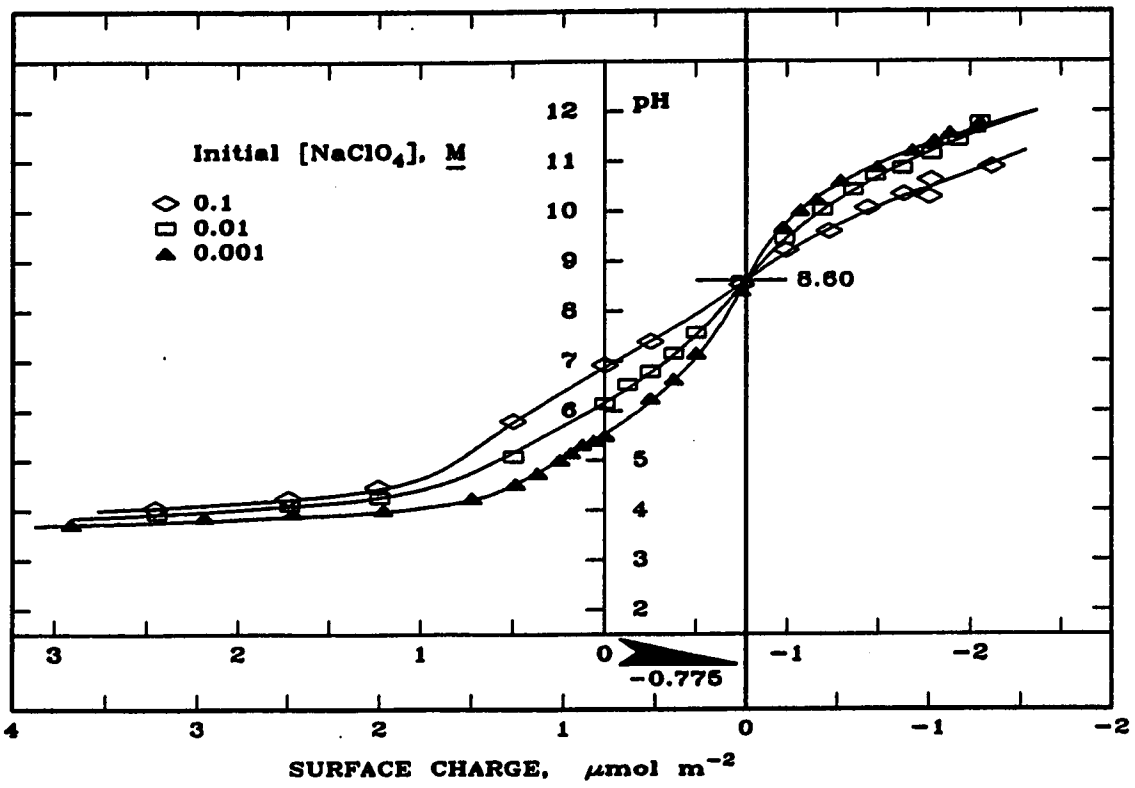

Fig. 2-2. Surface charge vs. pH of γ-Al_2O_3 at various ionic strengths using theoretical reference curves. Produced from batch titration data (Fig. 2-1) and Eq. [2.3].

Method II uses an electrolyte solution of $NaClO_4$, in concentrations equivalent to those used for the sample titrations, as the reference curve. The open symbols in Fig. 2-3 show the resulting titration curves of the reference electrolyte solutions. For comparison with method I, the solid line in Fig. 2-3 (labeled T) shows the resulting pH values if $(C_A - C_B)_{ref} = (H^+ - OH^-)_{ref}$. The solid line and the electrolyte solution titration curves are almost identical emphasizing the indifference of the electrolyte solutions towards the acid or base additions. At a given pH value, the difference between the reference curve (from Fig. 2-3) and the corresponding sample curve (from Fig. 2-1) yields surface charge vs. pH curves (Fig. 2-4). As expressed earlier by Eq. [2.8], the pH value where the curves intersect each other is the ZPC.

Equation [2.2] itemizes the negative and positive charges expected to be present in the system studied. However, Eq. [2.2] is not complete due to the γ-Al_2O_3 colloid partially dissolving and introducing Al species into the solution phase. The actual form and concentration of the dissolved Al is pH dependent. To complete Eq. [2.2], knowledge of the solubility of the colloid and speciation of the dissolved species is required. This information is not always easy to obtain and small errors are often not acceptable.

If a proper reference is chosen which contains an adequate sample of the species in solution, then subtracting the sample curve from the reference curve at

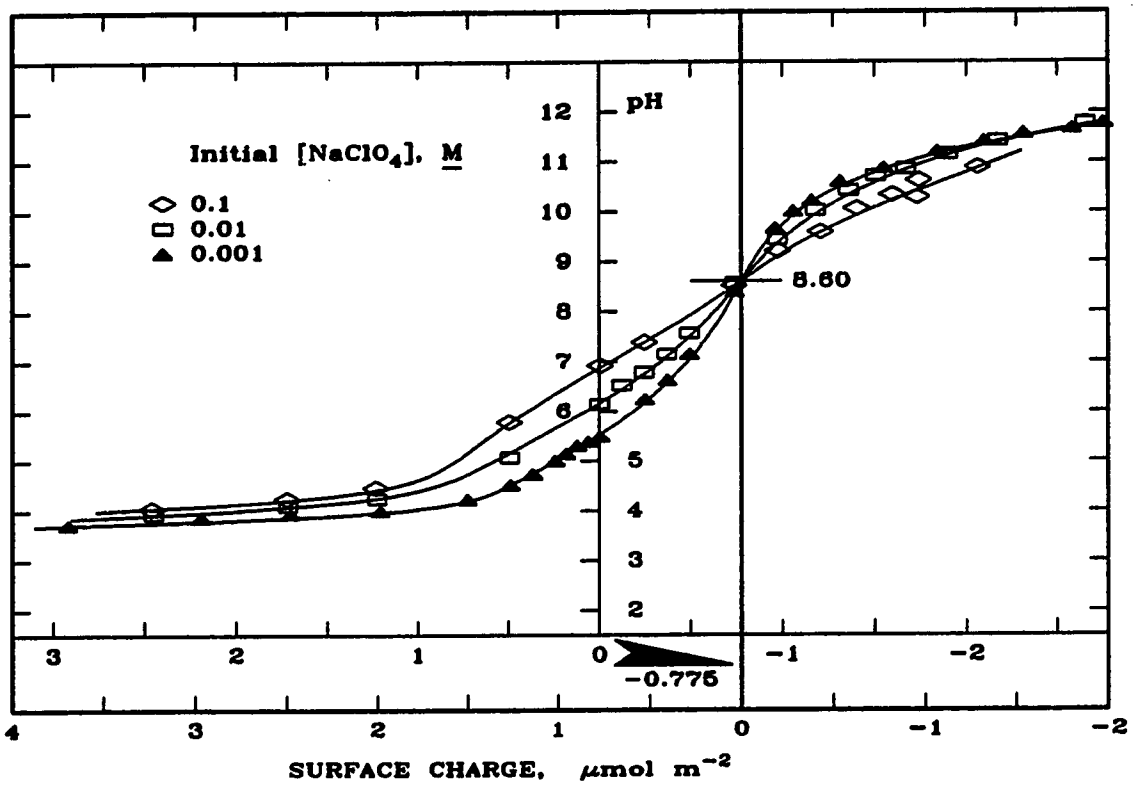

Fig. 2-4. Surface charge vs. pH of γ-Al_2O_3 at various ionic strengths using electrolyte titration reference curves. Produced from batch titration data (Fig. 2-1) and electrolyte titration curves (Fig. 2-3) using Eq. [2.11].

a given pH value would also yield Eq. [2.11]. In method III the reference chosen was the ZPT supernatant, or the colloidal suspension with zero acid or base additions. The solid symbols in Fig. 2-3 show the titration of the supernatant solutions at various ionic strengths. Subtracting the sample curves (from Fig. 2-1) from the corresponding supernatant curves (from Fig. 2-3) also produce surface charge vs. pH relationships (Fig. 2-5).

Surface charge analyses using methods I, II, and III resulted in very similar convex curves; the ZPC is at pH 8.60. According to Eq. [2.11], the pH of ZPC should coincide with the surface charge value equal to zero. Instead, the curves intersect at -0.775 μmol m^{-2} for methods I and II, and at -0.725 μmol m^{-2} for method III. Huang (1981) comments that if the intersection is located in the alkaline region of the titration, then there is specific cationic adsorption taking place. If the intersection is located in the acidic region, then there is specific anionic adsorption taking place. Finally, if the pH of ZPC is at $\sigma_o = 0$, then there is no specific adsorption of electrolytes present. The possibility of specific cationic adsorption exists for all three methods used in this study.

However, these methods are not free of problems. Each titration curve has an undetermined amount of error. Subtracting a sample titration curve from its corresponding reference curve compounds the errors present. Thus, since all the results are nearly the same, method I is preferred over method II or III. At

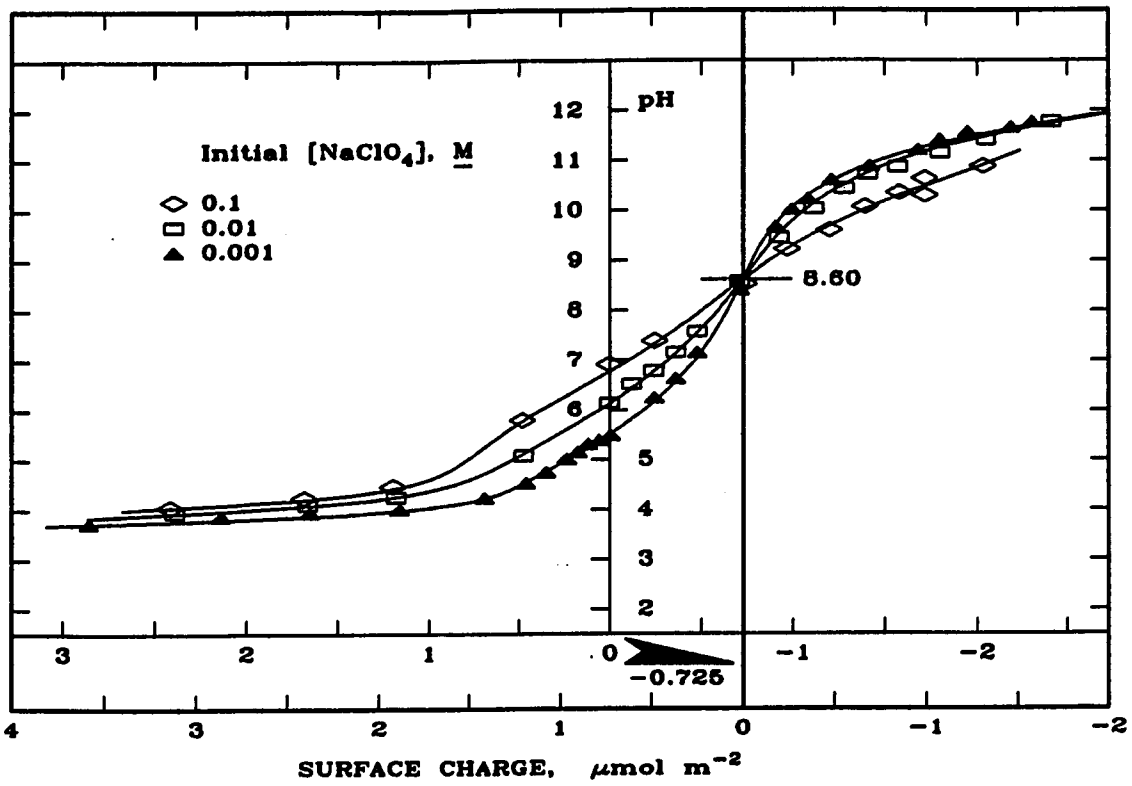

Fig. 2-5. Surface charge vs. pH of γ-Al_2O_3 at various ionic strengths using ZPT supernatant titration reference curves. Produced from batch titration data (Fig. 2-1) and ZPT supernatant titration curves (Fig. 2-3) using Eq. [2.11].

the pH of ZPC, the interference due to variations in electrolyte concentrations in the solution is assumed to be minimal. The interference due to solubility of the sample will also be at a minimum at the pH of ZPC (Parks and de Bruyn, 1962). Therefore, it is not recommended that a reference solution be subtracted from the sample titration curve if the ZPC value is the only parameter desired.

Some recent applications of singular reference curve methods are cited below. Beyrouty et al. (1984) determined ZPC for synthetic aluminum hydroxides by observing the ZPC value to be at the intersection of the batch oxide titration curves at various KCl electrolyte concentrations. Though the electroneutrality equation was not applied directly, their procedure was essentially similar to method I. Hendershot and Lavkulich (1979) applied method II for ZPC values of 10 Canadian soils using NaCl as the indifferent electrolyte. Barrow et al. (1980) applied method II for surface charge analysis and ZPC determination of a synthetic goethite (FeOOH), using some precautions to avoid CO_2 interferences. Huang and Stumm (1973) determined surface charge and intrinsic acidity constants for a γ-Al_2O_3 via method III. Their ZPC was 8.50, and intrinsic acidity constants were estimated with pK_a^{int} values of 7.9 and 9.1.

[2.3.2] Backtitration Technique (Method IV)

The graphical solutions to Eq. [2.1] used in methods II and III are still inadequate. The surface charge behavior analyses showed that the colloidal

surface charge increases to extremely high negative or positive values (Fig. 2-2, 2-4, and 2-5). This is not realistic since the surface cannot accommodate such large charges. Lyklema (1968) points out a contradiction between surface charge observations and electrokinetic behavior of Si and Fe oxides. The solution to this problem lies in properly defining the system.

The solubility of the γ-Al_2O_3 was not properly accounted for in method III. It is pH dependent, and various concentrations of Al in solution exert different effects on the shape of the colloidal titration curve shown in Fig. 2-1. The titration of an acidic supernatant (labeled A) is different from the titration of a basic supernatant (labeled B), both of which are shown in Fig. 2-3 for I = 0.001 *M*. Both A and B are also different from the titration of the ZPT supernatant shown by the solid symbols in Fig. 2-3. Parker et al. (1979) observe that the dissolution of Al would consume H^+ ions without affecting the surface charge.

Method IV treats each sample individually. The reference of each sample is the supernatant of the particular sample studied. All possible species existing in the aqueous phase will form part of the reference. Each supernatant is backtitrated to a common end point, and the mmol consumed is the alkalinity or acidity of the aqueous phase. Subtracting the sample's acid (or base) concentration from the concentration of base (or acid) used in the backtitration will yield the amount of acid (or base) consumed by the surface. Stumm and Morgan (1981) give a rigorous

analysis of alkalimetric and acidimetric titration curves. The "phenolphthalein end point" is at pH values near 8.3, but lowers with increasing amounts of soluble Al in solution (down to 7.9) or with increasing CO_2 loss to the atmosphere during titration (down to 7–7.3). The end point used for each run was fixed at pH 7.00 for simplicity since few analytical errors were observed using this value. Equation [2.9] was applied to balance the amount of acid (or base) added with the amount of base (or acid) consumed by the supernatants. Hohl and Stumm (1976) also employed a similar procedure to determine the maximum exchange capacity of a γ-Al_2O_3. They did not, however, run the procedure at various pH values. They also subtracted the calculated dissolved Al concentration which is not necessary since the backtitration takes this value into account.

Figure 2-6 shows the H^+ adsorption values obtained. The various ionic strength runs intersect at a pH value of 7.50 with a H^+ desorption value of 0.85 μmol m^{-2}. This point will be considered the PZSE for this particular system studied. This is close to the intersection value observed with the "singular reference curve" methods discussed earlier.

At higher ionic strength the curves in Fig. 2-6 are flattened, but they still follow closely the low ionic strength curve. These shifts are probably not due to compression of the double-layer, but rather due to the competitive behavior of the Na^+ ions with H^+ ions, and ClO_4^- ions with OH^- ions. At high Na^+

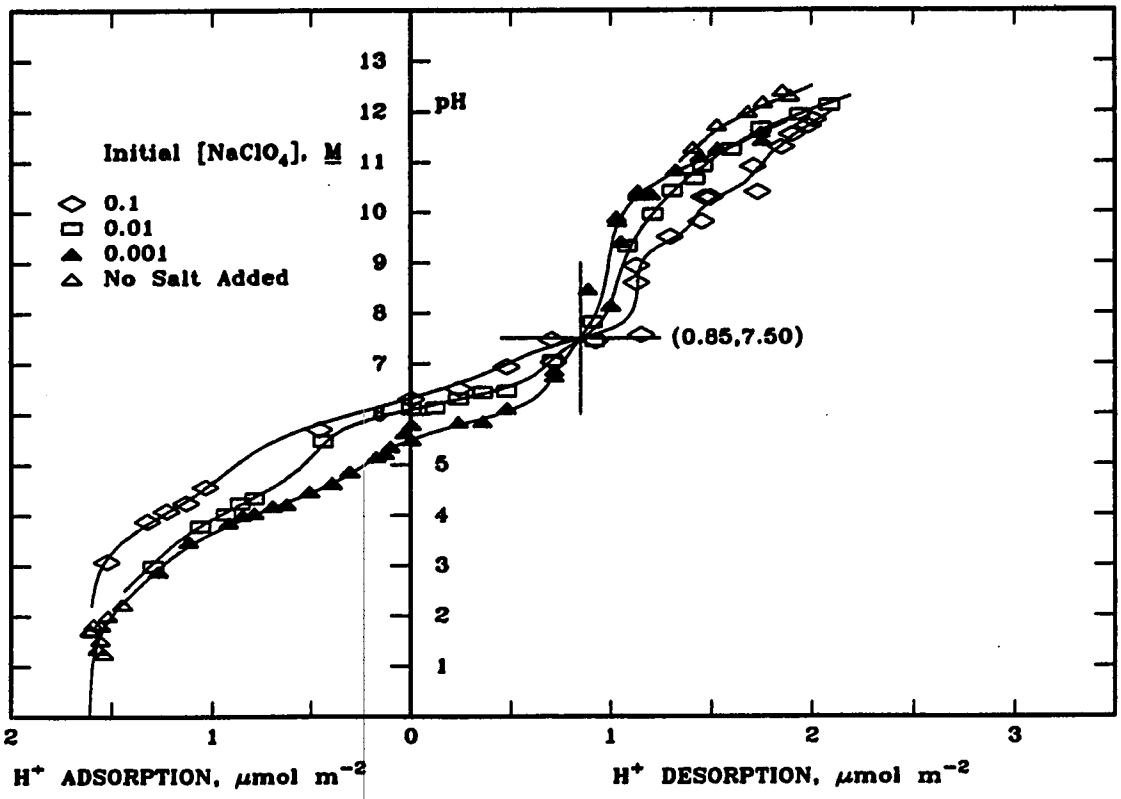

Fig. 2-6. Apparent adsorption or desorption of H^+ ion on γ-Al_2O_3 at various ionic strengths vs. pH of supernatant using the backtitration technique. Produced from batch titration data (Fig. 2-1) and backtitration to pH $\bar{7}$ for each data point using Eq. [2.9].

concentrations, if a Na^+ ion is specifically adsorbed competitively over a H^+ ion, then the figure would show an increase in apparent H^+ desorption. At high ClO_4^- concentrations, if a ClO_4^- ion replaces a OH^- ion on the colloidal surface by an anion exchange phenomenon, then the figure would show an increase in apparent H^+ adsorption. Each OH^- ion removed from the surface by anion exchange would neutralize a H^+ ion in solution and this would not be readily distinguished from H^+ ion removal by adsorption. Thus, at the PZSE the amounts of H^+ and OH^- displaced from the surface sites are equal in magnitude and no apparent change in pH is detected with changes in the salt concentration. The electrolytic reactions may be shown schematically as follows

$$\gamma\text{-}Al_2O_3 \text{ Surface} \begin{cases} \equiv OH + Na^+ = \equiv ONa + H^+ \\ \equiv OH + ClO_4^- = \equiv ClO_4 + OH^- \end{cases} . \qquad [2.12]$$

This is in agreement with Perrott et al. (1976) who found for several soils that the amount of OH^- released by NaF was dependent on pH and salt concentration, and that this correlated well with the amount of Al present in the soils. Ferris and Jepson (1975) found that adsorption of Cl^- and Na^+ on gibbsite ($Al_2O_3 \cdot 3H_2O$) varied dramatically with pH.

The magnitude and position of the observed breaks are currently being studied. The proton isotherms observed in Fig. 2-6 may be described in terms of speciation of the oxide surface with respect to pH. However, a proton sorption model would be needed to properly interpret the data. The problem arises in

that the ZPC is not the same as the PZSE, the surface charge is not equivalent to the proton isotherms, and the high ionic strength data shown in Fig. 2-6 may be only an apparent proton isotherm due to cation and anion competition. The presence of titration breaks, plateaus, and maximum adsorption capacities (as observed at the low pH values, and assumed also present for the high pH values) are characteristics which emphasize the presence of unique adsorption sites, and their interaction with the solution phase.

It should also be noted that the underlying assumption of the backtitration technique and the singular reference curve methods is that the missing charge in the solution phase must be present on the surface studied so as to maintain electroneutrality in the system. The singular reference curve methods assume that the surface charge and proton sorption are equivalent. This assumption may prove to be controversial in view of the preliminary results observed in Fig. 2-6.

[2.4] CONCLUSIONS

A ZPC of 8.60 was determined for the γ-Al_2O_3 that we studied. This value is defined as the pH value where surface positive and negative charges are equal, and was determined experimentally by titration analyses.

The purpose of subtracting a reference titration curve from the sample titration curve is to graphically solve Eq. [2.1] so as to maintain electroneutrality.

If a proper reference is chosen, then the resulting curve should be an isotherm of surface charge vs. pH. The theoretical solution to Eq. [2.1] produces very high positive and negative values (Fig. 2-2). When the reference chosen is the electrolyte solution in which the solid phase is suspended, the resulting isotherm is also convex at high and low pH values (Fig. 2-4). This was also observed when the reference chosen was the supernatant of the sample of zero acid or base additions (Fig. 2-5). None of these three singular reference curve approaches show definite titration breaks, nor are they realistic at extreme pH values.

To properly adjust for the changes in solubility of the γ-Al_2O_3 as the pH changes, a backtitration technique specific to each sample was found to more accurately reveal the adsorption behavior of H^+ on the colloidal surface (Fig. 2-6). The Na^+ ions are assumed to compete with H^+ ions for the adsorption sites while the ClO_4^- ions are assumed to undergo anion exchange with the surface–OH groups. A PZSE value of 7.50 was determined for the colloid. Though a sorption model is not yet developed which will allow one to make further conclusions, the presence of titration breaks and maximum adsorption capacities emphasize the presence of unique adsorption sites.

CHAPTER 3

TWO-SITE MODEL for ALUMINUM OXIDE with MASS BALANCED COMPETITIVE pH+SALT/SALT DEPENDENT REACTIONS

[3.1] INTRODUCTION

The adsorption of dissolved substances on a solid phase (charcoal) was accidentally discovered in 1785 by J. T. Lowitz (Figurovsky, 1973). A. L. Lavoisier (1743–1794) advanced a chemical, rather than mechanical, theory for the phenomenon of adsorption (Figurovsky, 1973). Modeling of the surface chemistry of oxides, colloids, or soils, has long been recognized by researchers as essential in optimizing crop yields, soil productivity, or the efficiency of any system requiring an interaction with a solid phase. Adsorption models were initially intended to describe gas adsorption by solids, and have been applied with some success to

aqueous adsorption. The most famous contribution was made by Langmuir (1918), whose equation may be easily derived for cation adsorption onto an oxide surface site. Assuming the following surface reaction

$$SOM \rightleftharpoons SO^- + M^+ \qquad [3.1]$$

where S is the surface of the solid phase, one can then define the corresponding equilibrium constant, K, as

$$K = \frac{\{SO^-\}(M^+)}{\{SOM\}} . \qquad [3.2]$$

The mass balance condition is then

$$\Gamma_{max} = \{SO^-\} + \{SOM\} \qquad [3.3]$$

where Γ_{max} = total number of sites,

$\{SOM\} = \Gamma_{M^+}$ = concentration of sites adsorbing M^+,

$\{SO^-\}$= concentration of sites lacking M^+, and

$(M^+) = c$ = bulk solution equilibrium concentration of M^+ .

Combining Eq. [3.2] and [3.3] gives

$$\Gamma_{max} = \frac{\{SOM\}}{k(M^+)} + \{SOM\} = \{SOM\}\left[\frac{1 + k(M^+)}{k(M^+)}\right] \qquad [3.4]$$

where $k = 1/K$. Rearranging one finds that

$$\frac{\Gamma_{M^+}}{\Gamma_{max}} = \frac{kc}{1 + kc} . \qquad [3.5]$$

Equation [3.5] is the Langmuir adsorption isotherm, and is often applied to cation and anion adsorption modeling (Olsen and Watanabe, 1957; Huang and Stumm, 1973). The concentration parameters should be expressed as activity values.

If the cation in question is H^+, the assumption is made that the proton becomes progressively more difficult to remove with each incremental removal of protons or degree of titration (Huang, 1981). Equation [3.2] is redefined in terms of an intrinsic equilibrium constant

$$K^{int} = \frac{\{SO^-\}(H^+)\exp(-F\Psi_o/RT)}{\{SOH\}} . \qquad [3.6]$$

The exponential term in Eq. [3.6] assumes that the surface charge causes a change in reactivity between the ions at the surface and in the bulk solution, which is described by the Boltzmann distribution (Barrow, 1985). The K^{int} value is then the acidity constant in a completely chargeless environment (Huang, 1981). Another hypothesis assumes the existence of a porous gel layer with an exponential decay of porosity capable of adsorbing ions (Lyklema, 1968; Romm and Rubashkin, 1985), which also results in an exponential adjustment to the H^+ ion concentration sorbed on the surface. In the presence of a divalent cation, the intrinsic equilibrium constant has been defined as (Barrow, 1985)

$$K^{int} = \frac{\{SOM^+\}(H^+)\exp(-F\Psi_s/RT)}{\{SOH\}(M^{2+})\exp(-2F\Psi_\beta/RT)} . \qquad [3.7]$$

Equation [3.7] is derived from a multilayer model that assumes the inner layer (s) to adsorb H^+ and OH^- ions, and the second layer (β) to adsorb the electrolyte ions.

It is not clear why the H^+ ion should be treated differently than any other ion. The "correction" in Eq. [3.6] does allow for exponential fitting of the convex behavior of surface charge vs. pH (σ_o-pH) curves. The assumption of two separate potentials for each layer and corresponding exponential corrections in Eq. [3.7] also allows for exponential fitting of the σ_o-pH curves. There are many models from which to choose (Barrow, 1985; Westall and Hohl, 1980), and they all fit σ_o-pH curves fairly well. Sposito (1983) observed that "these surface complexation models are *too* successful". However, there is insufficient proof as to which model is more realistic, or as to why the Boltzmann distribution correction term is necessary. Sposito (1984) discusses that equations similar to Eq. [3.6] should be formulated for metal surface reactions that result in a charged surface; however, he also states that very small or negligible dependence on the exponential terms for metal surface reactions are observed in practice.

Potentiometric titration curves adhere to the principle of electroneutrality that, upon rearrangement of the electroneutrality terms, yields an equation of mass conservation. The σ_o-pH curves are based on the same principle of mass conservation that cation and anion isotherms are based; i.e.,

$$\text{mass adsorbed} = \text{mass added} - \text{mass recovered} . \qquad [3.8]$$

Chapter 2 argued that Eq. [3.8] has not been properly applied to proton isotherm analyses due to the solubility of the solid phase, which is pH-dependent. Applying a backtitration technique, a proton isotherm was obtained that showed maximum

adsorption limits, distinct plateaus, and titration breaks. These observations were radical in that the assumptions used for Eq. [3.6] no longer apply. That is, the proton isotherm is not convex, and does not need to be fitted by exponential correction terms. It is strongly suggested that the exponential term in Eq. [3.6] is merely tracking the solubility behavior of the solid phase.

The Langmuir isotherm is a special case of the more general mass balanced set of equations; specifically, a single site with only one reaction assumed. In this chapter, a backtitration analysis of an Al oxide was made with the intention of presenting a proton isotherm model based on mass balanced equations, without assuming a variable stability constant with increasing degree of titration (i.e., $K = K^{int}\exp[F\Psi_o/RT]$ will not be assumed). The objectives of formulating a model were to (i) establish a definition, or interpretation, of the point of zero salt effect (PZSE) value obtained by the backtitration technique (Chapter 2), (ii) interpret the effect of the electrolyte concentration on the amount of proton adsorption, and (iii) advance a discussion on the validity of zero point of charge (ZPC) definitions determined through traditional singular reference curve methods (Chapter 2).

[3.2] MATERIALS and METHODS

The Al oxide studied was a γ-Al_2O_3 made by the Degussa Corp. of Teterboro, NJ, under the name of Aluminum Oxide C®. The oxide was acid washed with $HClO_4$ at pH 4.2, followed by an H_2O wash. The H_2O used was purified through an ultrapure D8902 cartridge (Barnstead Co., Newton, MA) and N_2 purged for at least 15 min before each use. The oxide was then washed with NaOH at pH 10.4 and a conductivity value of 0.362 S m^{-1}, followed by 12 H_2O washings to a final pH of 7.4 and a conductivity value of 840 μS m^{-1}. With each wash the sample was agitated overnight on a reciprocating shaker, and separated for 30 min on a RC-5B Sorvall centrifuge (DuPont Co., Wilmington, DE) at 40000 g for the acid suspensions, or 2000 g for the alkaline suspensions. After centrifuging and discarding the supernatant, the oxide was scraped from the centrifuge tubes and re-agitated with fresh solution. Tiny dark spots ($\approx$ 1%) were noticed on the centrifuge tubes, particularly after the acid washings, and were removed from the oxide sample whenever possible. A N_2 atmosphere was maintained at all times, except during the removal of the oxide from the centrifuge tubes.

After the 12 H_2O washings, the sample was again resuspended in H_2O and used as the stock Al oxide suspension for all experiments. Approximately 1 L of stock solution was prepared and found to have a density of 84.06 g L^{-1} and a specific surface area, as described by Heilman et al. (1965) using ethylene glycol monomethyl ether (EGME), of 83.1 m^2g^{-1}. Before the sample was washed, the

initial surface area by EGME was 95.0 m^2g^{-1}; this value compared well with the surface area by BET (see Brunauer et al., 1938) of 100±15 m^2g^{-1} supplied by the manufacturer. The objective of all these washings was to obtain an Al oxide suspension that was free of unknown impurities.

The adsorption behavior of H^+ ions on the Al oxide was determined by mass balance as outlined in the backtitration technique of Chapter 2. The procedure was modified by adding 5 mL of Al oxide suspension to 30 mL of pH/electrolyte concentration adjusted water. The pH was adjusted with known quantities of either 0.24 *M* HCl or 0.24 *M* NaOH; the electrolyte used was NaCl. The total volume on all samples was 35 mL. The exclusion volume was estimated to be 0.145 mL; thus, the total initial aqueous volume was set equal to 34.855 mL for the backtitration technique calculations. Another run was made with 15 mL of Al oxide suspension and 20 mL of pH adjusted water, with no salt additions. After equilibrating overnight, centrifuging and filtering through 0.2-μm GA-8 Gelman filter paper, the weighed supernatant was backtitrated to pH 8.00 with either 0.03 *M* NaOH or 0.03 *M* HCl.

Prior to backtitrating, some samples were analyzed for Cl^- or Na^+ concentration remaining in solution. The Cl^- ion concentration was analyzed with an Orion Cl^- ion selective electrode; the Na^+ ion concentration was analyzed on a Perkin Elmer 5000 Atomic Absorption spectrometer buffered with LiCl to minimize flame induced ionization problems.

[3.3] MODEL DEVELOPMENT

There are two aspects to a model: (i) a physical interpretation, and (ii) a mathematical interpretation. The physical model is intended to help conceptualize the effects exerted on the oxide's surface. The mathematical model is usually the core of the discussion, and it is based here entirely on mass balanced equations. The assumed parameters controlling the transitions of one surface structure to another (mathematical aspect) are independent of the assumptions on what the surface structure actually looks like (physical aspect).

[3.3.1] Basis for a Two-site Model

The more types of sites that are assumed in a model, the greater the number of mathematical parameters available for controlling the behavior of predicted values. However, it is essential that a model, and each of the mathematical parameters, have a physical counterpart to maintain meaning and correspondence with reality. The emphasis here is therefore placed on the chemical nature of Al. With a valence of +3, each edge Al can support two amphoteric surface–OH groups and still remain bonded to the solid phase. For Al, a model involving more than two sites per surface Al atom would be difficult to conceptualize.

[3.3.2] Determination of Γ_{max}

Two values are needed in determining the maximum amount of ions each site can adsorb: the total number of protons adsorbed at the extreme pH values, Γ_{TOTAL}, and the amount adsorbed to reach an assumed neutral condition, Γ_o. The backtitration technique in proton isotherm analysis of an oxide should show a clear maximum amount of adsorbed H^+ at very low pH values, or a maximum amount desorbed at very high pH values. At high pH, negative adsorption values denote either OH^- adsorbed, or H^+ desorbed. Electrokinetic studies reviewed by Parks (1965) give ZPC values of 8.0 for Al oxides. With Γ_o as the value obtained at pH 8.0, the maximum amount sorbed per site, Γ_{max}, is

$$\Gamma_{max} = \frac{\Gamma_{TOTAL} - \Gamma_o}{\text{no. of site types}} . \qquad [3.9]$$

[3.3.3] CO_2 Adsorption

Even with the precautions taken in using an ultrapure ion exchange cartridge and N_2 gas during the oxide washings to purge CO_2 from the system, CO_2 would still be able to adsorb on the oxide during the brief transfers from the centrifuge tubes, particularly at high pH values. Martin and Smart (1987) observed through x-ray photoelectron spectroscopy (XPS) that C contamination existed on all the goethite (α-FeOOH) surfaces that were exposed to air. The presence of CO_2(aq) in the system is therefore considered an active species that can adsorb/desorb

from the solid phase. Though the author was not able to obtain literature on CO_2 adsorption on Al oxides, the following model was assumed

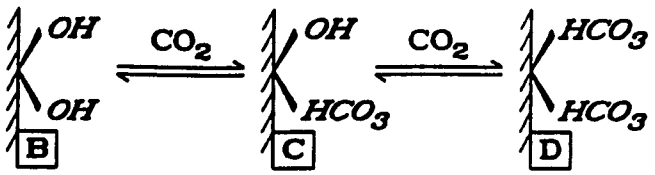

[3.10]

In a closed system, species *B* would exist at a higher pH than *C* or *D*. Higher CO_2(aq) concentrations would be expected at lower pH values in a closed system (Stumm and Morgan, 1981), which would in turn increase equilibrium towards CO_2 adsorption on the Al surface. In an open system, CO_2(aq) concentration would be constant and pH-independent (Stumm and Morgan, 1981). Caution should be taken not to confuse CO_2(aq) with total carbon, $(CO_2)_{TOTAL} = (H_2CO_3) + (HCO_3^-) + (CO_3^{2-}) + (CO_2)aq$.

[3.3.4] pH Dependent Reactions: Effects and Limitations

The adsorption and desorption of H^+ ions on a two-site model may be depicted by

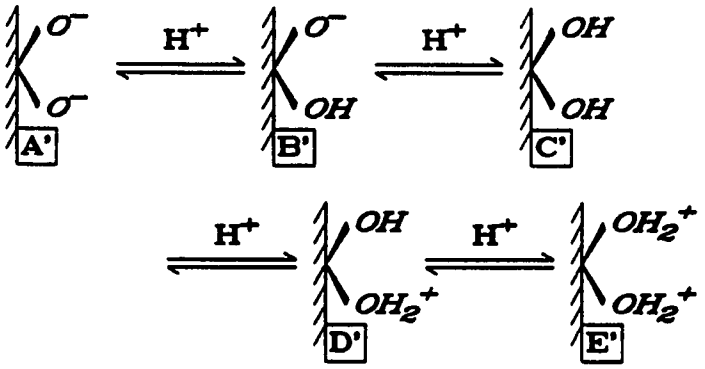

[3.11]

Species A' would exist at very high pH values, C' at the pH of ZPC, and E' at very low pH values. To model Eq. [3.11], four equilibrium constants (K) and a mass balance condition are needed. The pK values ($-\log K$) used are determined by fitting the curve to the data with no initial NaCl additions. Four plateaus are generated by this model, and the center of each plateau corresponds to 50% of each species involved in the transition. The pK value for each transition controls the location of only one of the plateaus, moving it up or down like elevators. This type of model does not have a parameter that would allow the predictions to vary with changes in the initial electrolyte concentration; i.e., only one line can be generated when plotting adsorption vs. pH.

[3.3.5] pH+Salt Dependent Reactions

The positive and negative charges that develop on the oxide surface shown on Eq. [3.11] are balanced by counterions in the bulk solution. However, if the adsorption of counterions is stoichiometrically related to the adsorption of protons, then there is sufficient reason to incorporate the concentration of the counterions into the model; specifically, in the definition of the equilibrium constants. With the assumption that each transition is dependent on the pH and salt concentration of the bulk solution, the model then would generate a different line for each initial salt concentration when plotting adsorption vs. pH. Again, the pK value for each transition controls the location of one of the plateaus. The assumed equilibrium

constants were

$$\text{high pH,}\quad K_a = \frac{\{\text{SOH}\}(\text{OH}^-)(\text{Na}^+)}{\{\text{SONa}\}},$$

$$K_b = \frac{\{\text{SHCO}_3\}(\text{OH}^-)^2}{\{\text{SOH}\}},$$

$$\text{low pH,}\quad K_c = \frac{\{\text{SHCO}_3\}(\text{H}^+)(\text{Cl}^-)}{\{\text{SCl}\}}\ . \qquad [3.12]$$

These reactions may be explained as two simultaneous steps. At high pH, the OH^- anion neutralizes the surface–OH proton forming H_2O and a negative surface, and the Na^+ cation satisfies the charge imbalance. Similarly, at low pH, the H^+ cation reacts with the surface–HCO_3 group to form H_2CO_3 and a positive surface, and the Cl^- anion satisfies the charge imbalance. For the surface–HCO_3 group, the transitions shown in Eq. [3.10] are also assumed to involve two-step reactions, with the surface–HCO_3 to surface–OH transition resulting in two OH^- anions removed from the bulk solution.

It is worthwhile to note that the following two species cannot be differentiated by the potentiometric methods used

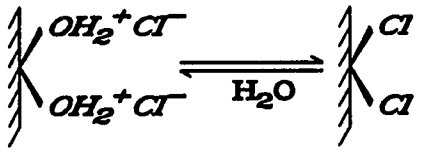

[3.13]

The oxide surface on the right is the one used in this chapter since it emphasizes that the Cl^- anion is an active species in the surface reactions.

[3.3.6] Competitive Salt (pH-independent) Reactions

A set of exchange reactions may also be assumed based on the salt concentrations only, with secondary neutralizing reactions taking place in the bulk solution. For example, a Cl^- anion may exchange with a surface–OH (or -HCO_3) group, with the reaction dependent only on the Cl^- concentration. The exchanged OH^- (or HCO_3^-) would in turn consume H^+ ions in the bulk solution. Similarly, the Na^+ cation may exchange with the proton of a surface–OH group. The HCO_3^- and CO_2(aq) concentrations were ignored in all of the competitive reactions; the reactions were assumed to be dependent on Na^+ or Cl^- concentrations only. The assumed equilibrium constants were

$$K_d = \frac{\{SOH\}(Na^+)}{\{SONa\}}, \quad \text{and} \quad K_e = \frac{\{SHCO_3\}(Cl^-)}{\{SCl\}} . \qquad [3.14]$$

A reaction that consumes (or releases) H^+ ions in the bulk solution should also be pH-dependent. However, the data obtained by the backtitration technique is a result of two reactions: first there is the titration-induced aqueous/surface reactions, followed by the aqueous backtitration reactions. Equation [3.14] describes the equilibrium constant for those reactions that have had the pH-dependent characteristics presumably factored out by the backtitration procedure. Equation [3.12] describes the equilibrium constant for those reactions that have remained both pH and salt-dependent after the backtitration procedure.

The equilibrium constants described by Eq. [3.14] generate vertical lines, or pH-independent values, on proton adsorption vs. pH plot analyses. Changes in the salt concentrations result in changes in the amount of H^+ consumed in the bulk solution (which cannot be distinguished from H^+ adsorbed on the surface). The pK values for these transitions control the sensitivity of the reaction response to changes in the salt concentrations.

[3.4] APPLICATION of MODEL

[3.4.1] Stoichiometric Considerations

Figure 3-1 shows the adsorption isotherms of H^+, Na^+, and Cl^- ions for the samples with 0.0 and 0.001 M initial NaCl concentrations. The isotherms were determined by mass balance (Eq. [3.8]) and by the backtitration technique (Chapter 2). Similar patterns were obtained at higher initial electrolyte concentrations; however, the scatter on the Cl^- isotherm was greatly increased due to the difficulty in detecting very small concentration differences at high electrolyte concentrations. The Na^+ cation was removed from solution at pH>10, and correlates well with the H^+ desorption pattern. However, at pH>11.8 the Na^+ ion removal was too large and follows a convex pattern. This suggested an error in the determination of Na^+ ions in the bulk solution. It was hypothesized that the Na^+(aq) complexed with the dissolved $Al(OH)_4^-$(aq) and thus avoided detection by atomic absorption spectroscopy. This would cause the recovered

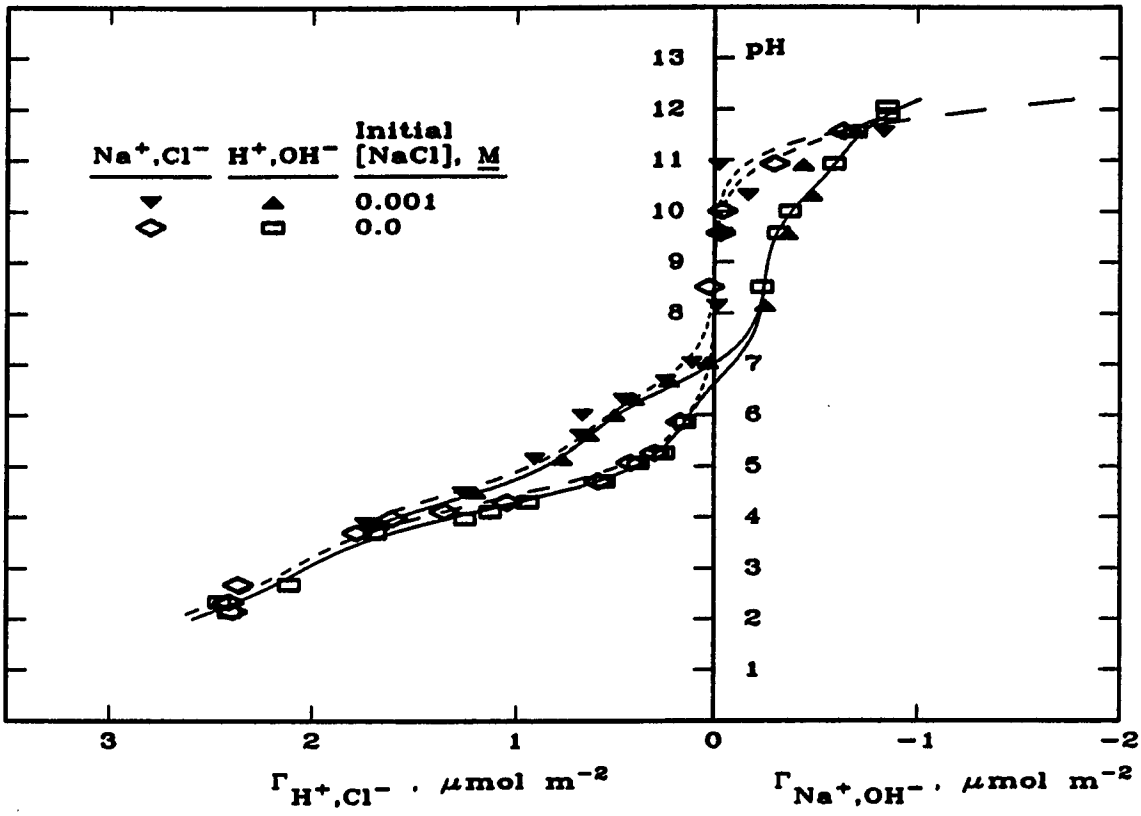

Fig. 3-1. Proton and NaCl adsorption isotherm on Al oxide. Key: (□) proton adsorption with no initial NaCl additions; (△) proton adsorption with 0.001 *M* NaCl added; (◇) Cl^- ion adsorption (pH<8), or Na^+ cation adsorption (pH>8), with no initial NaCl additions; (▽) Cl^- ion adsorption (pH<8), or Na^+ cation adsorption (pH>8), with 0.001 *M* NaCl added. Proton isotherms traced with solid lines; Na^+ and Cl^- isotherms traced with dashed lines. [Al oxide]=0.4203 g/35 mL.

Na^+ concentration to be underestimated. It was immediately noticed that these independent measurements yield nearly identical results, particularly the Cl^- isotherm and the H^+ isotherm. These observations were central to the development and application of the model in that they established a 1:1 correlation between the salt and H^+ ion removal from solution. It therefore follows that the model should not only predict the H^+ isotherm, but also the removal of salt ions from solution.

[3.4.2] Determination of Γ_{max}

Figure 3-2 shows the proton isotherm for the samples containing 1.2609 g of Al oxide with a maximum at 3.15 μmol m^{-2} of H^+ adsorbed (Γ_{TOTAL}) at the low pH values. At the high pH values the maximum is not distinct, and it appears that H^+ ions may still be released at higher pH values. There is definitely no convex shape to these curves. The isotherm is shifted by -0.25 μmol m^{-2} (Γ_o) at pH 8.0, and Eq. [3.9] gives a displacement of 3.4 μmol m^{-2} ($= \Gamma_{TOTAL} - \Gamma_o$). A two-site model, therefore, yields a maximum amount of adsorption per site (Γ_{max}) of 1.7 μmol m^{-2}. This is equivalent to 0.977 $nm^2 site^{-1}$ of surface Al containing two active site types of 0.488 nm^2 each.

[3.4.3] Determination of pK Values

Based on the results shown in Fig. 3-1, it was assumed that all surface reactions must involve a Cl^- anion (or Na^+ cation), and thus the ion concentration

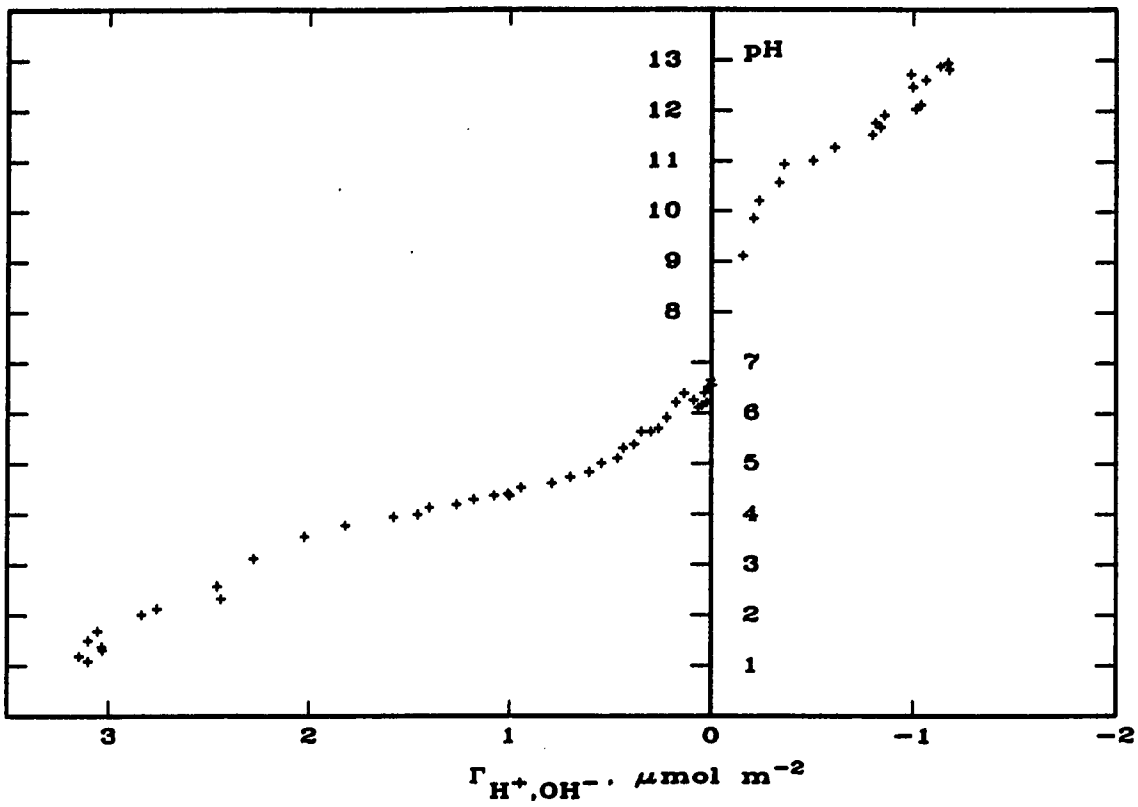

Fig. 3-2. Proton adsorption isotherm on Al oxide. [Al oxide]=1.2609 g/35 mL with no initial NaCl salt present.

was incorporated in the equilibrium equations. The Cl^- and Na^+ concentrations used in the equations were calculated from the sum of the constituent sources:

$$(Cl^-)_{eq} = (NaCl)_{added} + (HCl)_{added} - (Cl^-)_{adsorbed} \quad [3.15]$$

$$(Na^+)_{eq} = (NaCl)_{added} + (NaOH)_{added} - (Na^+)_{adsorbed} \cdot \quad [3.16]$$

The loss due to adsorption is determined by an iteration procedure. It is important to note that it is impossible to add H^+ cations without Cl^- anions (conjugate base), or OH^-anions without Na^+ cations (conjugate acid). Thus, to generate a prediction on the amount of protons adsorbed at a given pH, the amount of acid or base added had to be known. If no data were available at a given pH, the trapezoidal rule was applied to estimate the amount that would be added. The concentrations were expressed as activities; the ion activity coefficients (γ) were determined with the Güntelberg equation (Stumm and Morgan, 1981):

$$\log \gamma = \frac{-0.5z^2\sqrt{I}}{1+\sqrt{I}} \quad [3.17]$$

where I= ionic strength, and z= valence of the ion.

The assumed pH+salt-dependent reactions are illustrated vertically in Fig. 3-3, and the corresponding equilibrium constants are assumed to be dependent on one pH term (H^+ or OH^-), and one salt term (Na^+ or Cl^-, but may also be OH^-again); see Table 3-1 for definitions of K_1 to K_5. The transitions $B \rightleftharpoons C \rightleftharpoons D$ (Fig. 3-3) are presumed to consume H^+ ions only in the bulk solution. This gives one H^+ desorbed for each species A formed, one H^+ adsorbed for each species E

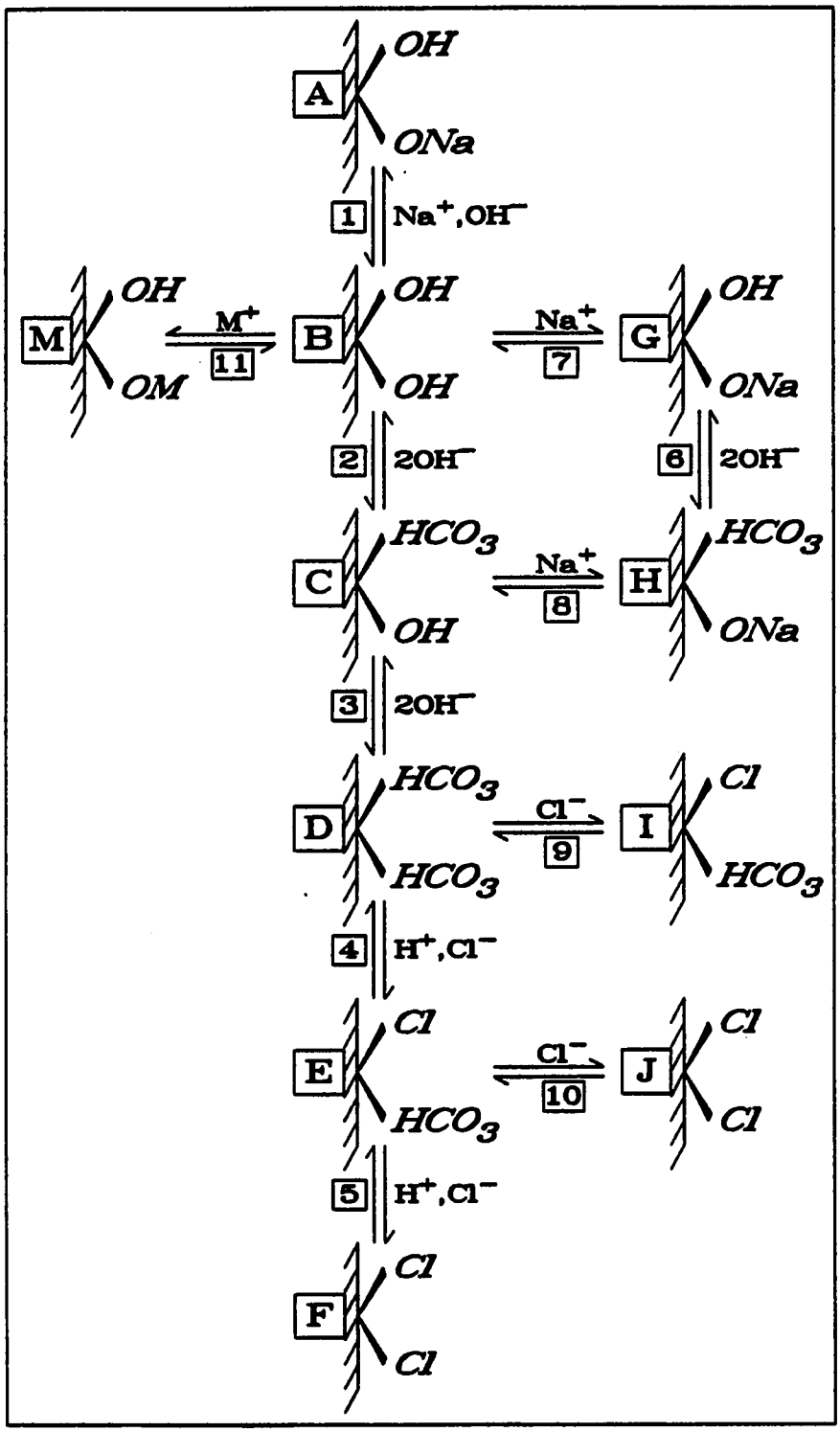

Fig. 3-3. The competitive pH+salt/salt-dependent reactions for Al oxide.

Table 3-1. The equilibrium constants for the surface Al oxide reactions; $pK = -\log K$.†

Equilibrium constants	pK	Reaction no.
$K_1 = \frac{\{A\}}{\{B\}(Na^+)(OH^-)}$	−3.2	[1]
$K_2 = \frac{\{B\}}{\{C\}(OH^-)^2}$	−8.5	[2]
$K_3 = \frac{\{C\}}{\{D\}(OH^-)^2}$	−15.5	[3]
$K_4 = \frac{\{D\}(H^+)(Cl^-)}{\{E\}}$	7.5	[4]
$K_5 = \frac{\{E\}(H^+)(Cl^-)}{\{F\}}$	4.2	[5]
$K_6 = \frac{\{G\}}{\{H\}(OH^-)^2}$	−8.5	[6]
$K_7 = \frac{\{B\}(Na^+)}{\{G\}}$	1.2	[7]
$K_8 = \frac{\{C\}(Na^+)}{\{H\}}$	0.5	[8]
$K_9 = \frac{\{D\}(Cl^-)}{\{I\}}$	3.0	[9]
$K_{10} = \frac{\{E\}(Cl^-)}{\{J\}}$	1.6	[10]
$K_{11} = \frac{\{B\}(M^+)}{\{M\}}$	2.8	[11]

† Braces $\{i\}$ are activity of surface species i shown in boxes next to corresponding oxide surface in Fig. 3-3. Parentheses (i) are activity of species i in bulk solution. The subscripts correspond to reaction numbers shown in boxes in Fig. 3-3.

formed, and two H^+ adsorbed for each species F formed. Likewise for the Cl^- anion, species E and F correspond to one and two Cl^- adsorbed, respectively. Each pK value (Table 3-1, [1]–[5]) was determined one at a time and all the other reactions were ignored. These pK values control the location of the plateaus, and the values were chosen based on the best fit of the curve corresponding to the data with no initial NaCl additions. The resulting curves (Fig. 3-4) greatly underestimated the data for high electrolyte concentrations, but this was to be expected without the incorporation of the salt-dependent reactions.

By studying the data shown in Fig. 3-4, it becomes apparent that there must also be a pH-independent reaction involved in the model. It is easy to see the pH-dependent behavior (proton adsorption not present at high pH, and proton desorption not present at low pH), but a pH-independent behavior is also shown. In Fig. 3-4, between pH 5 and 7, there are adsorption maxima reached whose values depend on the salt concentration present. The same thing is observed in various parts of the graph: between pH 2 and 3, 8 and 9, and 10 and 11. Therefore, competitive pH-independent reactions have been introduced into the model. The hypothesized reactions are shown in Fig. 3-3 with the pH+salt-dependent reactions drawn vertically and the pH-independent reactions drawn horizontally.

The pK values for the salt-dependent reactions were also determined one at a time; the pH+salt-dependent reactions and their respective pK values previously

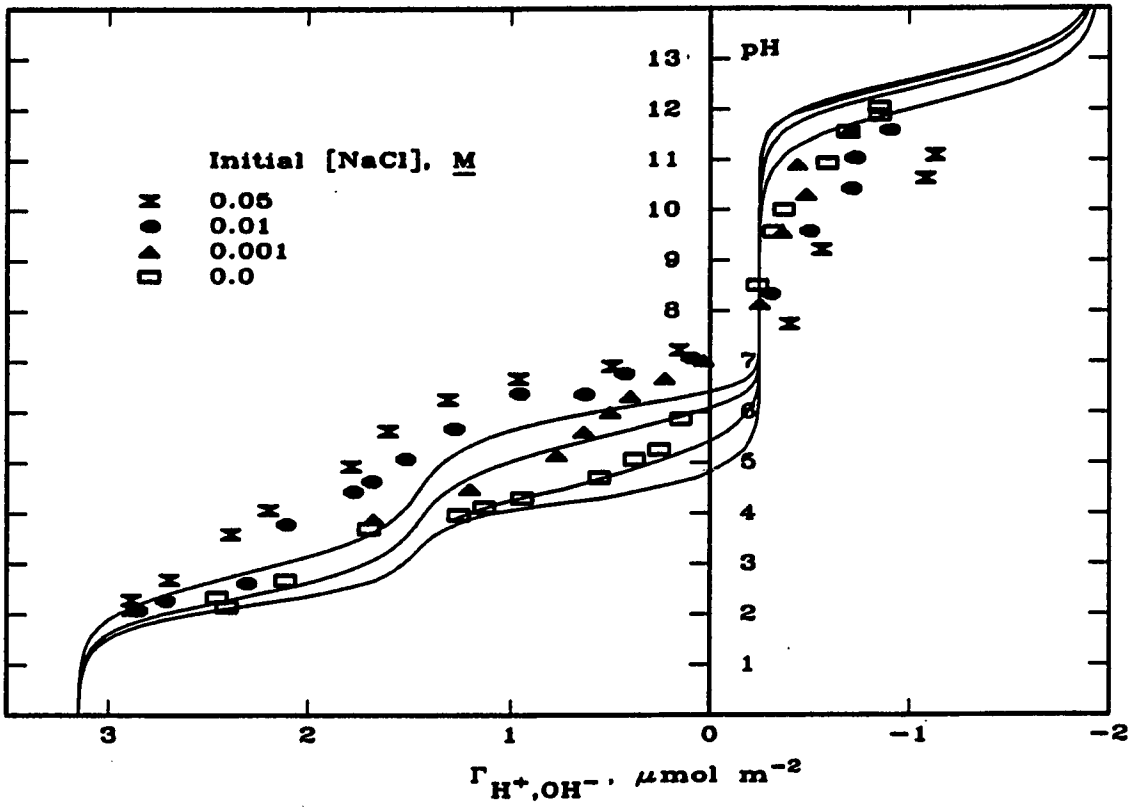

Fig. 3-4. Proton adsorption isotherm on Al oxide with predicted values of pH+salt model. The solid lines drawn are the predicted values for several initial NaCl concentrations; [Al oxide]=0.4203 g/35 mL.

determined were not ignored. For the pH range 5 to 7, the hypothesized Cl^- anion dependent reaction (Table 3-1, [9]) is essentially a substitution reaction of Cl^- for HCO_3^-. The pK_9 value was calculated based on the best fit of the data. The same procedure and hypothesis were applied for the pH range 2 to 3 (Table 3-1, [10]). For the pH range 8 to 9, and 10 to 11, the competitive Na^+ ion dependent reactions are assumed to be substitution reactions of Na^+ for H^+. These pK values (Table 3-1, [7]–[8]) were determined by the best fit with the high initial NaCl concentration data. An important observation was made in trying to fit the alkaline data: The competitive products must be interconnected by pH+salt-dependent reactions. Without these connections (Table 3-1, [6]) the predicted values would reverse themselves. For example, if Reaction 6 is ignored, then the model would predict proton desorption at pH>8 (due to some formation of species H), proton desorption reversal at pH>8.5 (due to formation of neutral species B, and depletion of species H), followed by proton desorption at pH>9.5 (due to some formation of species G). These reversals do not occur as long as the competitive products are connected. Since these pK values cannot be fitted, they are assumed to be identical to the paralleled reactions; e.g., pK_6 = pK_2.

The lines drawn in Fig. 3-5 show the predictions generated based on the pK values defined in Table 3-1 for the pH+salt/salt-dependent reactions just described.

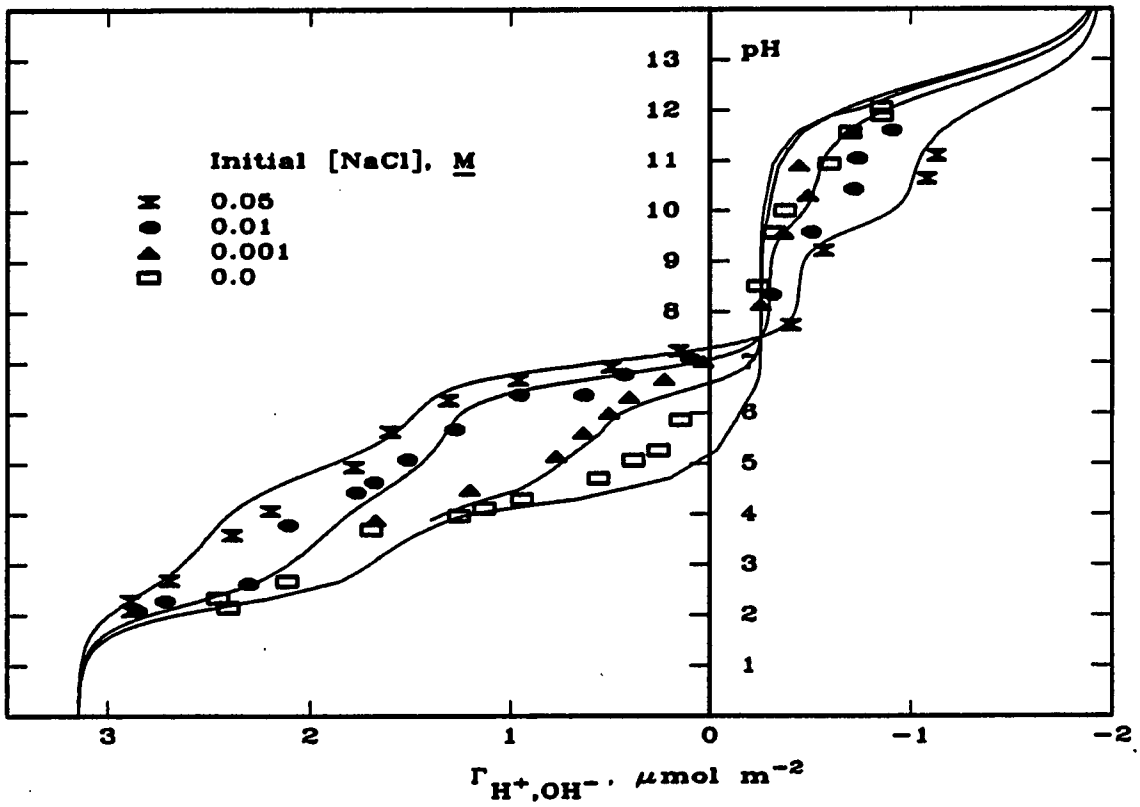

Fig. 3-5. Proton adsorption isotherm on Al oxide with predicted values of pH+salt/salt-competitive model (impurities ignored). The solid lines drawn are the predicted values for several initial NaCl concentrations; [Al oxide]=0.4203 g/35 mL.

[3.4.4] The Adsorption Shift: Impurity Effects

In Fig. 3-5, for the data with no NaCl additions, the model underestimates the amount of protons adsorbed in the slightly acidic pH range (5–7). To understand this discrepancy, note that the isotherm data for washed Al oxide differ from the unwashed Al oxide data previously reported (Chapter 2), particularly with respect to the amount of shift of the PZSE from the zero adsorption readings. Since the washings narrowed the amount of shift, it was assumed that any shift observed was due to initial salt impurities still remaining on the oxide surface after washing. The source of the salt may be from the oxide lattice itself, as well as from the product of the acid followed by base washings.

The Al oxide was manufactured by flame hydrolysis of anhydrous $AlCl_3$. The Degussa product quality control indicates <0.5% HCl may be present. For this reason, Cl^- anions are the presumed impurity that causes the negative PZSE shift. This is in contradiction with Huang (1981), who states that negative PZSE shifts are due to specific cation adsorption. However, assuming an initial Cl^- concentration of 0.0005 M due to impurities (determined by a best fit analysis), the model predictions are almost on target with all the data in the acidic range (Fig. 3-6).

In Fig. 3-5, the model also underestimates the amount of proton desorbed in the alkaline pH region (>9.5). Again, the reasoning is based on salt impurities.

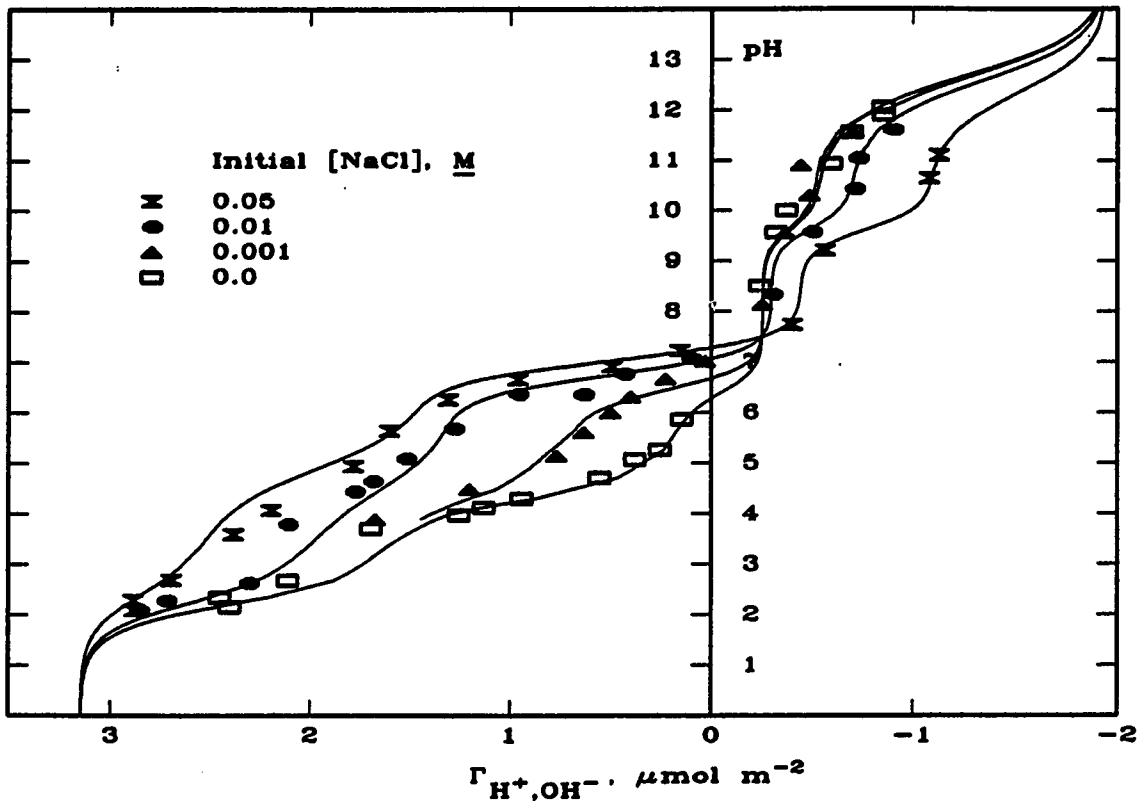

Fig. 3-6. Proton adsorption isotherm on Al oxide with predicted values of the pH+salt/salt-competitive model. The solid lines drawn are the predicted values for several initial NaCl concentrations with an estimated impurity of [MCl] = 0.0005 *M*; [Al oxide]=0.4203 g/35 mL.

However, there is no information as to what kind of cation may be present as an impurity. For the low initial NaCl additions, the model shown in Fig. 3-5 underestimates the data by an amount nearly equal to the PZSE shift. It was therefore assumed that the amount of cation (M^+) impurity present was equivalent to the amount of anion (Cl^-) impurity assumed earlier (0.0005 M). The M^+ cation may be related to the tiny dark spots observed during the washings.

Figure 3-3 illustrates the M^+ cation competing with the pH+salt-dependent reactions, just like the Na^+ cation. The pK value for this competitive metal reaction was determined by best fit of the data, and is shown in Fig. 3-6.

[3.4.5] Overview: Speciation of Surface

The proton isotherm shown in Fig. 3-6 was modeled based on the observations of five plateaus corresponding to five pH+salt-dependent reactions, and four adsorption shifts corresponding to four competitive salt-dependent reactions. Mathematical modeling of the reactions illustrated in Fig. 3-3 was based on the equilibrium constants shown in Table 3-1, and the following mass balance condition:

$$\{\mathrm{Al}\}_{\mathrm{TOTAL}} = \{A\} + \{B\} + \{C\} + \{D\} + \{E\} + \{F\} + \{G\} + \{H\} + \{I\} + \{J\} + \{M\} \; . \qquad [3.18]$$

Each species was defined in terms of a common species with the equilibrium

constants in Table 3-1. The speciation fraction, α_i, for each species was defined as the ratio Γ_i/Γ_{max} by

$$\alpha_i = n_i/D \qquad [3.19]$$

where $D = \sum n_i$, and the n_i values defined in Table 3-2. Note that $\sum \alpha_i \equiv 1.0$, and each surface speciation fraction may be independently determined given only the pH and the equilibrium salt concentration (Eq. [3.15]-[3.16]). The model finally predicts the proton adsorption isotherm by

$$\Gamma_{H^+,OH^-} = \Gamma_{max}(\alpha_I + \alpha_E + 2\alpha_J + 2\alpha_F - \alpha_A - \alpha_G - \alpha_H - \alpha_M) + (\text{Shift}) \qquad [3.20]$$

where $\Gamma_{max} = 1.7$ μmol m^{-2}, and Shift $= -0.25$ μmol m^{-2}. It should be emphasized that the data were not force fitted. Force fitting involves at least one independent empirical parameter that cannot be experimentally determined. All the pK values were obtained by best fit with the data, but there were no empirical parameters involved. All concentration values used in the model were experimentally confirmed. An exception is the (M^+Cl^-) impurity concentration, which may be improved upon in future model revisions. The existence of the M^+Cl^- impurity, however, is strongly suggested by the visual observation, the manufacturing procedure, and by the decrease in the amount of shift of the PZSE from the zero adsorption readings after washing the oxide.

Table 3-2. Numerator values, n_i, for determining surface speciation fractions, α_i.

$n_A = K_1K_2K_3(\mathrm{Na^+})(\mathrm{OH^-})^5$	$n_G = \left(\frac{K_6K_3}{K_8} + \frac{K_2K_3}{K_7}\right)(\mathrm{Na^+})(\mathrm{OH^-})^4$
$n_B = K_2K_3(\mathrm{OH^-})^4$	$n_H = \frac{K_3(\mathrm{Na^+})(\mathrm{OH^-})^2}{K_8}$
$n_C = K_3(\mathrm{OH^-})^2$	$n_I = \frac{(\mathrm{Cl^-})}{K_9}$
$n_D = 1$	$n_J = \frac{(\mathrm{H^+})(\mathrm{Cl^-})^2}{K_4K_{10}}$
$n_E = \frac{(\mathrm{H^+})(\mathrm{Cl^-})}{K_4}$	$n_M = \frac{K_2K_3(\mathrm{M^+})(\mathrm{OH^-})^4}{K_{11}}$
$n_F = \frac{(\mathrm{H^+})^2(\mathrm{Cl^-})^2}{K_4K_5}$	

Figure 3-7 shows the speciation of the Al oxide surface for various initial electrolyte concentrations as a function of pH. Species M, A, G, and H all consume one OH^- anion, and are summed under the -1 curve in Fig. 3-7. Species B, C, and D are neutral, and are summed under the 0 curve. Species I and E consume one H^+ ion, and are summed under the +1 curve. Finally, species J and F consume two H^+ ions and are summed under the +2 curve. The removal of Na^+ cations are also summed under the -1 curve, and the removal of Cl^- anions are also summed under the +1 and +2 curves. Two vertical lines are drawn in Fig. 3-7 that indicate the pH of two surface conditions: negative=positive surface concentration, and maximum concentration of neutral surface sites. The former always occurred at lower pH values than the latter.

[3.5] RESULTS and DISCUSSION

The intersection of the curves in Fig. 3-6 at pH 7.5 is the PZSE, and Fig. 3-7 shows that it coincides with the surface condition of H^+ adsorption equivalent to H^+ desorption (or, H^+ consumed = OH^- consumed). Technically, Fig. 3-7 shows that the PZSE decreases with increasing electrolyte concentration (7.76–7.50). However, in Fig. 3-6 it is the high ionic strength (I) curves that are visibly seen intersecting the other curves at pH 7.50 (or, at the pH of PZSE for the high I curves). The amount of Cl^- adsorbed is also equivalent to the amount of Na^+ adsorbed at the PZSE, based on Fig. 3-1 and on the stoichiometric relationship

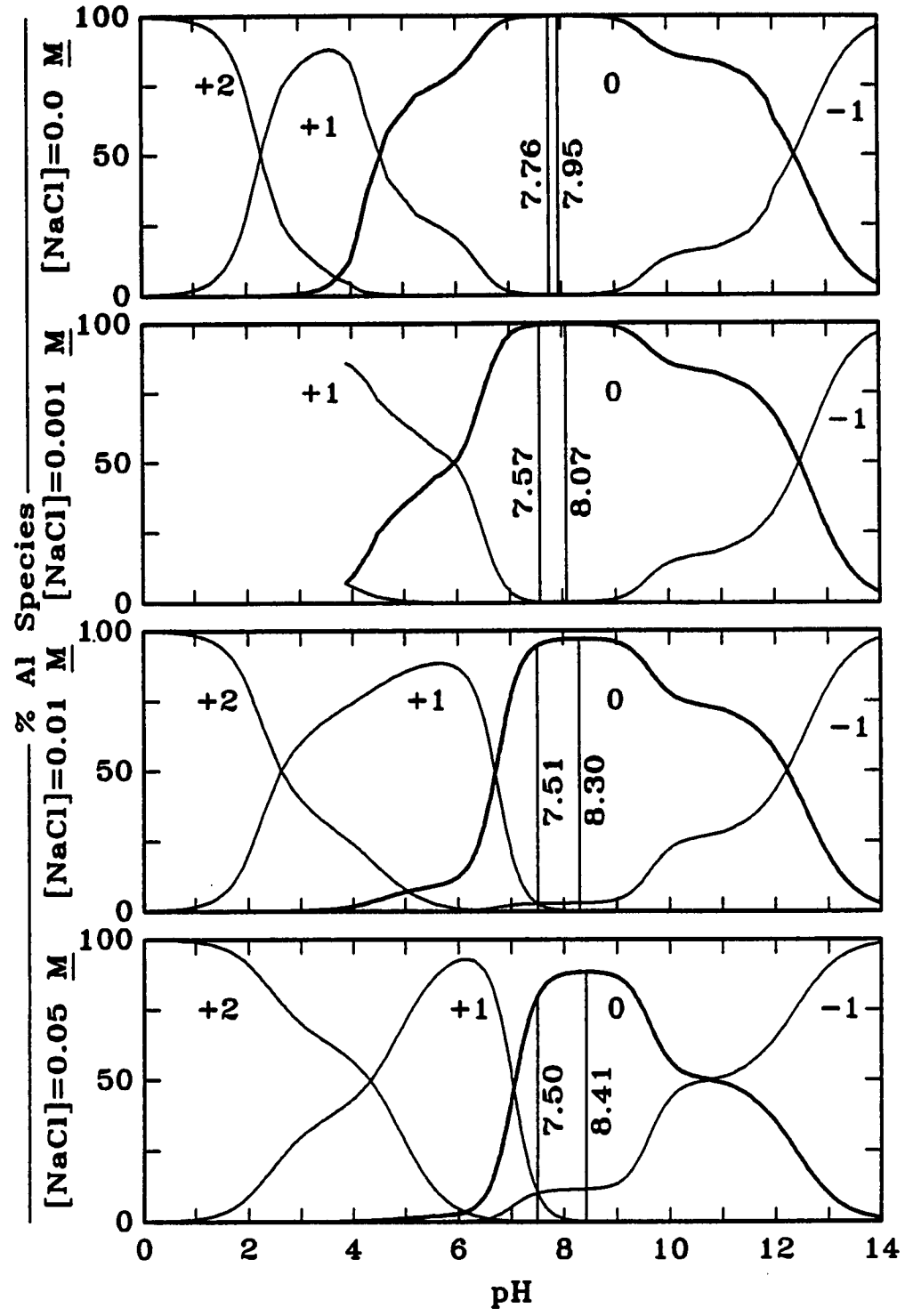

Fig. 3-7. The surface speciation of the Al oxide.

assumed in the proposed model. It is emphasized that the proton isotherm, and the cation and anion isotherms, are stoichiometrically related. The term *point of zero net charge* (PZNC) has been suggested for the condition of cation exchange capacity = anion exchange capacity (CEC=AEC) (Sposito, 1984), and would therefore be equivalent to the PZSE; i.e., these two independently measured isotherms should agree on their respective neutral values or intersection points.

Figure 3-7 also shows that the maximum concentration of neutral surface sites falls at pH values >pH of PZSE (pH range 7.95–8.41, depending on the NaCl concentration). This emphasizes that *neutral surface conditions* are not equivalent to *maximum concentration of neutral sites*. The difference between them increases with the electrolyte concentration of the analysis.

A ZPC analysis of this washed Al oxide, using traditional potentiometric methods (Chapter 2), showed an intersection of the isotherms at pH 7.5 (Fig. 3-8). The reference used for this analysis was theoretical (singular reference curve method I) and the pH plotted was the supernatant pH. It was also observed that since the data tend to be in close proximity between pH 7 and 9, it is easy to misplace the ZPC value by as much as one pH unit. Thus, if sufficient data are collected near the pH of neutral surface conditions, the ZPC values obtained by singular reference curve methods are similar to the PZSE values obtained by the backtitration method. The advantages of the backtitration technique are primarily

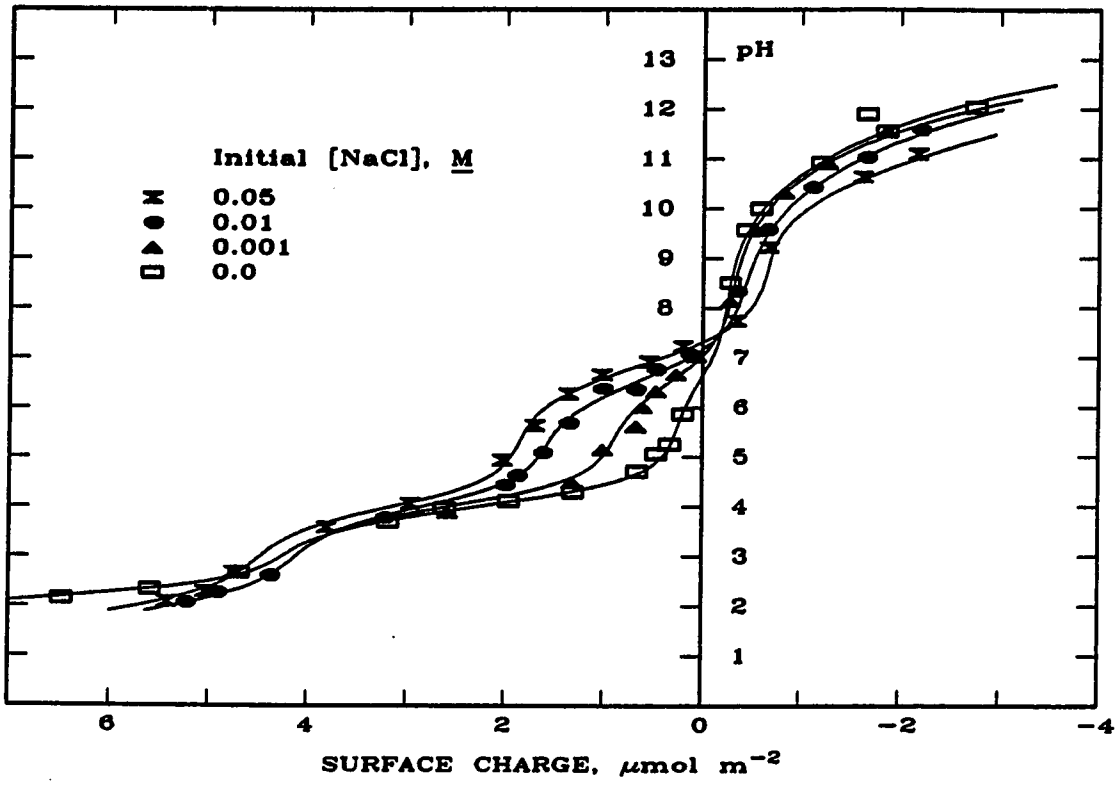

Fig. 3-8. ZPC analysis of the Al oxide (washed) using traditional potentiometric titration methods (singular reference curve method).

on the analyses of the proton isotherm. It is not clear at this time if the PZSE and ZPC values would agree in systems with multiple surface sites; this uncertainty is due to the variable solubility of each surface present.

The concept of competitive behavior also suggests that anion adsorption envelopes (Hingston et al., 1967, 1972) are merely an adsorption competition between the anion studied with all the other anions in the system. One should keep in mind that as acidic H^+ ions are added, anions are also added. The anion specificity is pH-dependent due to the competitive behavior of OH^- anions. If the anions in solution vary with pH, then the model is obviously more complex. However, for an anion such as F^-, the adsorption pattern is competing with OH^- anions at high pH values (right side of adsorption envelope), and also competing with Cl^- anions added as HCl at low pH values (left side of adsorption envelope). The presence of CO_2(aq) may also complicate any proposed model. Therefore, it is strongly recommended that if pH-dependent studies are performed, that the form of the acid or base used be clearly stated, and that the amount used be considered as a significant factor in the experiment.

[3.6] CONCLUSIONS

The proton isotherm behavior of an Al oxide can be successfully modeled with mass balanced equations. Intrinsic equilibrium constants and exponential terms were avoided due to an error in the development of these terms. A backtitration technique (Chapter 2) was used to collect the proton isotherm data, and was found to be stoichiometrically related to the cation and anion isotherm behavior. The assumed model was based on: (i) two surface sites, (ii) pH+salt-dependent reactions (H^+ and Cl^-, $2OH^-$, or Na^+ and OH^-), (iii) competitive salt-dependent reactions (Na^+ or Cl^-), (iv) CO_2(aq) pH-dependent reactions with the surface–OH groups, and (v) presence of an unknown M^+Cl^- salt (0.0005 *M*). The total number of Al sites was 1.7 μmol m^{-2} (equivalent to 0.977 nm^2site^{-1} of surface Al), or 3.4 μmol m^{-2} of total available sites. Figure 3-3 shows the assumed physical interpretations of the proposed model. The pH of PZSE represented the surface condition in which the negative charges (or cation surfaces) equaled the positive charges (or anion surfaces); the CEC equaled AEC at this value. The CEC–AEC data and proton isotherm data were stoichiometrically correlated. The pH of PZSE values ranged from 7.50 to 7.76 depending on the electrolyte concentration present, with lower values as the concentration increased. The initial presence of impurities on the surface studied will cause the intersection of the curves on the proton isotherm analysis to shift from the zero adsorption axis. Negative shifts are due to anion impurities adsorbed on the surface at initial experimental conditions:

conversely, positive shifts are due to cation impurities. These theories would also explain the anion adsorption envelope phenomena as the result of competitive anion reactions.

The ZPC intersection of the σ_o-pH curves generated by traditional potentiometric methods, or singular reference curve methods (Chapter 2), was found to coincide with the PZSE value of the backtitration method. However, since the singular reference curve methods do not account for the pH-dependent solubility of the surface, their resulting proton isotherms are not representative of the proton adsorption phenomena. The solubility effects greatly overshadow any adsorption phenomena, and it may be the solubility phenomena that is being tracked by the exponential terms in models involving intrinsic equilibrium constants.

CHAPTER 4

A CRITICAL ASSESSMENT

of

SURFACE ADSORPTION MODELS

[4.1] INTRODUCTION

Surface charge research by soil and colloidal scientists typically describe surface chemical reactions in terms of pH and surface potential (Ψ_o). Electrokinetic data confirm that surface potential is pH dependent, and electrostatic studies state that the surface potential varies linearly with surface charge (σ_o)

$$\sigma_o = C\Psi_o \qquad [4.1]$$

where C = capacitance density. Equation [4.1] is useful for colloid research if the colloidal particles are assumed to behave like capacitors, i.e., a constant capacitance model (Schindler and Gamsjäger, 1972).

Electrokinetics may involve either electrophoresis, electroosmosis, streaming potential, or sedimentation potential. The zeta potential measured by electrokinetics is the potential at the surface of the plane of shear, which in turn is influenced by the charge of the entire solid colloid up to the plane of shear. Electrokinetic measurements were recognized early in soil science as an important tool for understanding surface charge phenomena (Dayhuff and Hoagland, 1924; Mattson, 1926). A major hypothesis suggested by Arrhenius (1922), in which electrokinetics played an important confirming role, was that clays may act as an ampholyte. Electrokinetic research has since generally been reserved for investigating floc stability, predominantly with respect to its application in water treatment.

A limitation of electrokinetics is that no information on the number of surface sites per unit area is obtained. For this information the chemist resorts to potentiometric titration data. Since these titrations must adhere to the principle of electroneutrality, each proton adsorbed by the surface must increase surface charge by one equivalent charge unit. Thus, proton adsorption or desorption as determined by potentiometric analysis is generally considered synonymous with surface charge. There are, however, some inconsistencies that dramatically complicate this otherwise simple description of surface charge. First of all, potentiometric titration curves of soils yield no definite breaks to indicate end points. This problem was observed early in soil research by Bradfield (1923).

Another problem is that the surface charge predicted by potentiometric titration curves is extremely large at only a few pH units above and below the zero point of charge (ZPC). Though this inconsistency with the surface charge behavior as determined by electrokinetics was questioned by Lyklema (1968), it has been generally ignored.

Use of electrokinetics for describing surface charge characteristics has not been aggressively pursued in the soil science literature; instead, the charge behavior of a soil or oxide sample is usually characterized through potentiometric titration or cation-anion exchange methods. Unfortunately, each of these methods yields different results (Sposito, 1984) and have resulted in an array of zero point definitions and surface charge interpretations. The terms used are often methodology dependent and are, therefore, vague in their physical interpretations. The cation-anion exchange method has become an acceptable method in soil science following Schofield (1949). Chapters 2 and 3 show that the cation-anion exchange methods yield identical data to potentiometric titration methods if a backtitration technique is used. They argue that the traditional titration methods do not account for the solubility of the solid phase, which in turn acts as a significant source (or sink) for H_3O^+ ions in the titration procedure. Ignoring the solubility phenomena has resulted in a long list of questionable surface charge data and theories, as well as an array of zero point definitions.

This chapter shall review the limitations of adsorption models that are based on traditional potentiometric titration data. Furthermore, the electrokinetic behavior of an Al oxide will be compared with the proton isotherm behavior determined by the backtitration technique (Chapter 2). This is necessary to completely correlate the surface charge behavior as determined by the three methods mentioned above: cation-anion exchange, potentiometric titrations, and electrokinetics. The model used to describe the potentiometric titration data and the cation-anion exchange data in Chapter 3 will be shown to be also useful in describing electrokinetic data. The latter model does not use intrinsic equilibrium constants nor Boltzmann distribution terms as opposed to several other models that have been employed by soil chemists. Justification for not including these terms follows.

[4.2] MATERIALS and METHODS

[4.2.1] Theoretical Considerations

Potentiometric titration curves of soils yield no definite breaks to indicate end points, as is observed in the titration of liquid solutions. This inconsistency is ascribed to the basic assumption that the ionization of each surface site affects the acidity of the neighboring surface sites (Huang, 1981). The amount of work required to ionize the surface is further assumed to be related to the concentration ratio of the potential determining ion (PDI) based on the Boltzmann factor

(Hiemenz, 1977)

$$\frac{(H^+)_{SURFACE}}{(H^+)_{BULK}} = \exp\left(\frac{-w}{kT}\right) = \exp\left(\frac{-ze\Psi_o}{kT}\right) \quad [4.2]$$

where w= work required to bring the proton from the bulk solution to the surface with a potential Ψ_o, z= valence of ion, e= unit charge, and kT= energy terms. Another assumption that needs to be made is how to correlate surface charge (σ_o) to surface potential. The constant capacitance model (Eq. [4.1]) is often used, e.g., Goldberg and Sposito (1984); however, other models have been used, particularly the diffuse double-layer model from the Gouy-Chapman theory

$$\sigma_o = \sqrt{8\varepsilon\epsilon_o RTI}\,\sinh(F\Psi_o/2RT) \quad [4.3]$$

where ε= dielectric constant, ϵ_o= permittivity of free space, F= Faraday's constant, RT= energy terms, and I= ionic strength. Westall and Hohl (1980) were able to fit the surface charge data equally well using several models, including the constant capacitance model and diffuse double-layer model. The electrolytes used to adjust the ionic strength are also assumed to be indifferent; this assumption often also applies to the conjugate acid (Na^+) and base (Cl^-) introduced with the pH adjustments of the medium. Finally, assuming only two surface reactions

$$SOH \rightleftharpoons SO^- + H^+ \quad [4.4]$$

$$SOH + H^+ \rightleftharpoons SOH_2^+ \quad [4.5]$$

the theory on variable ionization energy states that the intrinsic equilibrium

constants may be defined as

$$K_b^{int} = \frac{\{SO^-\}(H^+)\exp(-F\Psi_o/RT)}{\{SOH\}} \quad [4.6]$$

$$K_a^{int} = \frac{\{SOH_2^+\}}{\{SOH\}(H^+)\exp(-F\Psi_o/RT)} \quad [4.7]$$

where S = surface, and all the values are in activities. The equations are then used to generate curves that predict surface charge vs. pH data obtained from a potentiometric titration analysis of the solid oxide.

Chapter 2 modified the traditional potentiometric titration procedures by backtitrating the supernatant solutions and correcting for the interfering solubility behavior of the solid phase. The resulting isotherms (H^+ removed vs. pH) were not convex, showed definite maximum values, and had clearly defined breaks to indicate end points. These observations seriously challenge the theory that the ionization energy of the surface sites vary with degree of titration. Chapter 3 later developed a surface speciation model based on mass balanced equations and constant ionization energy of the surface sites.

Solubility diagrams (–log[aq. species] vs. pH) of oxides and minerals confirm a logarithmic relationship between the solubility of the solid phase and the pH of the medium (see Stumm and Morgan, 1981). At pH values >pH of minimum solubility, the solubility usually increases 10-fold for each unit increase of pH; at pH values <pH of minimum solubility, the solubility sometimes increases 1000-fold

for each unit decrease of pH. The slope of the lines on the solubility diagrams are generally integer values (i.e., 1:1, 1:2, 1:3).

How does solubility affect potentiometric titration curves and surface charge analyses of oxides? First, the ZPC is near the pH of minimum solubility (Parks and de Bruyn, 1962). The exponential terms in Eq. [4.6] and [4.7] would be equal to 1.0 at the pH of ZPC ($\sigma_o = 0$, $\Psi_o = 0$). As the pH (or H^+ activity) changes, the remaining terms in Eq. [4.6] and [4.7] would also change so as to maintain the K^{int} values constant. Since the solubility of the solid phase has been ignored, the surface charge data is overestimated as follows:

$$\begin{aligned} \sigma_o &= \{SOH_2^+\}_{MEASURED} - \{SO^-\}_{MEASURED} \\ &= \{SOH_2^+\}_{TRUE} - \{SO^-\}_{TRUE} \pm [\text{Dissolved}] \; . \end{aligned} \qquad [4.8]$$

Parker et al. (1979) observe that the dissolution of Al would consume H^+ ions without affecting the surface charge. The aqueous phase reactions cannot be distinguished from the solid phase reactions, however, unless they are physically separated. Figure 4-1 illustrates this overestimation of surface charge. The σ_{TRUE} curve was from the data obtained in Chapter 3, and the dissolution effect was determined from a solubility analysis of the same data. (The degree of hydrolysis of Al in solution is easily obtained by potentiometric titration of the supernatant solution. The magnitude of the buffering capacity at pH 4.7 or 9.0 is directly related to the Al concentration present. For an illustration of this buffering capacity effect see Fig. 2-3). The net surface charge curve is also presented in

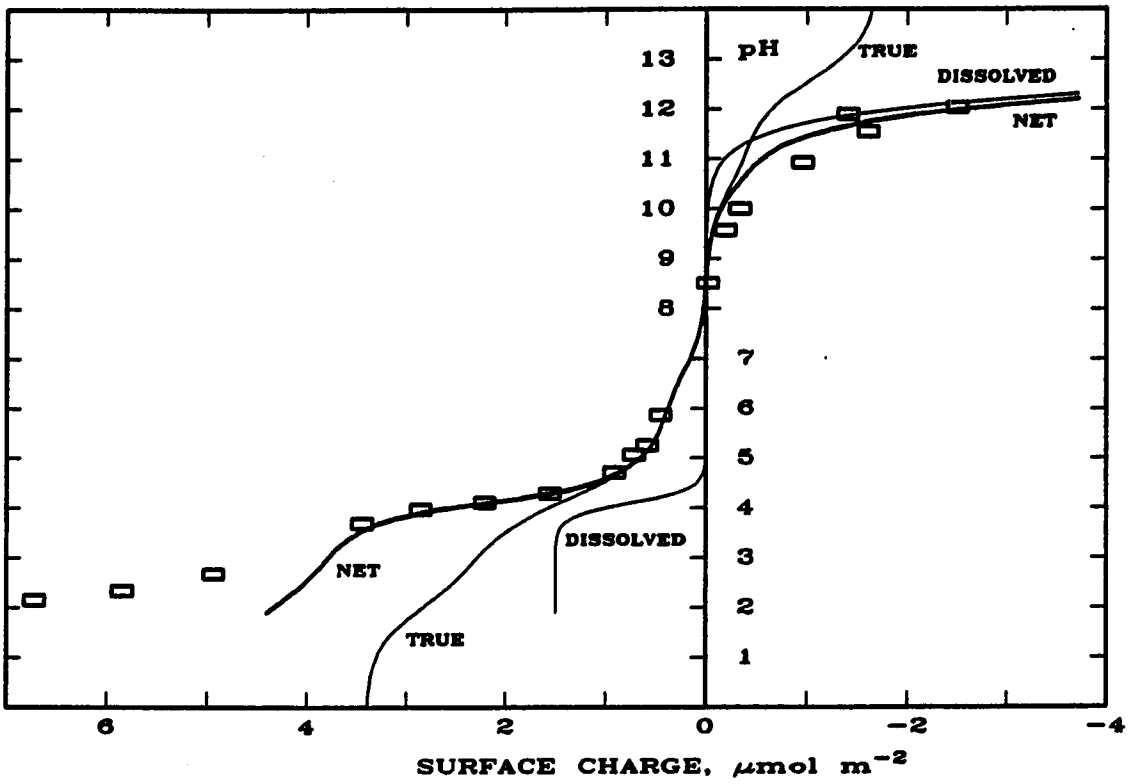

Fig. 4-1. Illustration of components of surface charge data (NET= TRUE + DISSOLVED). TRUE= potentiometric titration analysis (backtitration technique) from Chapter 3. DISSOLVED= apparent adsorption of protons due to dissolution of the Al oxide. The (□) symbols are surface charge values obtained by traditional potentiometric titration analysis (singular reference curve method). Note that the curve labeled TRUE also agrees well with cation-anion exchange data obtained in Chapter 3. Initial ionic strength was zero.

Fig. 4-1 along with the surface charge data using the traditional potentiometric titration method (viz., singular reference curve method I). The close match of the net (summation generated) surface charge curve with the traditional experimental data clearly proves that the singular reference curve method misrepresents the surface charge phenomena. This is particularly true in the alkaline region and at pH <4.5 for this Al oxide.

Van Riemsdijk et al. (1987) state, "it is not yet possible to identify the exact nature of all relevant surface complexes with spectroscopic techniques." Consequently, cation-anion exchange, potentiometric titration analyses, and electrokinetics are currently our best sources for elucidating the nature of the surface chemical reactions. The presence of buffered zones in potentiometric titration analyses are clear indicators that chemical reactions are taking place. These buffered zones are easily misinterpreted, however, when the methodology and theoretical analysis of the data ignore the solubility of the solid phase. By correcting for the solubility phenomena in Chapter 3, several distinct changes in the titration patterns were observed and subsequently modeled with several surface reactions (Fig. 4-2); on the other hand, if the solubility behavior remains unaccounted for, then the potentiometric titration data can be interpreted by only two surface reactions, such as Eq. [4.4] and [4.5], or even one surface reaction (e.g., van Riemsdijk et al., 1987). Ignoring the solubility of the solid phase causes a large distortion of the isotherm analyses.

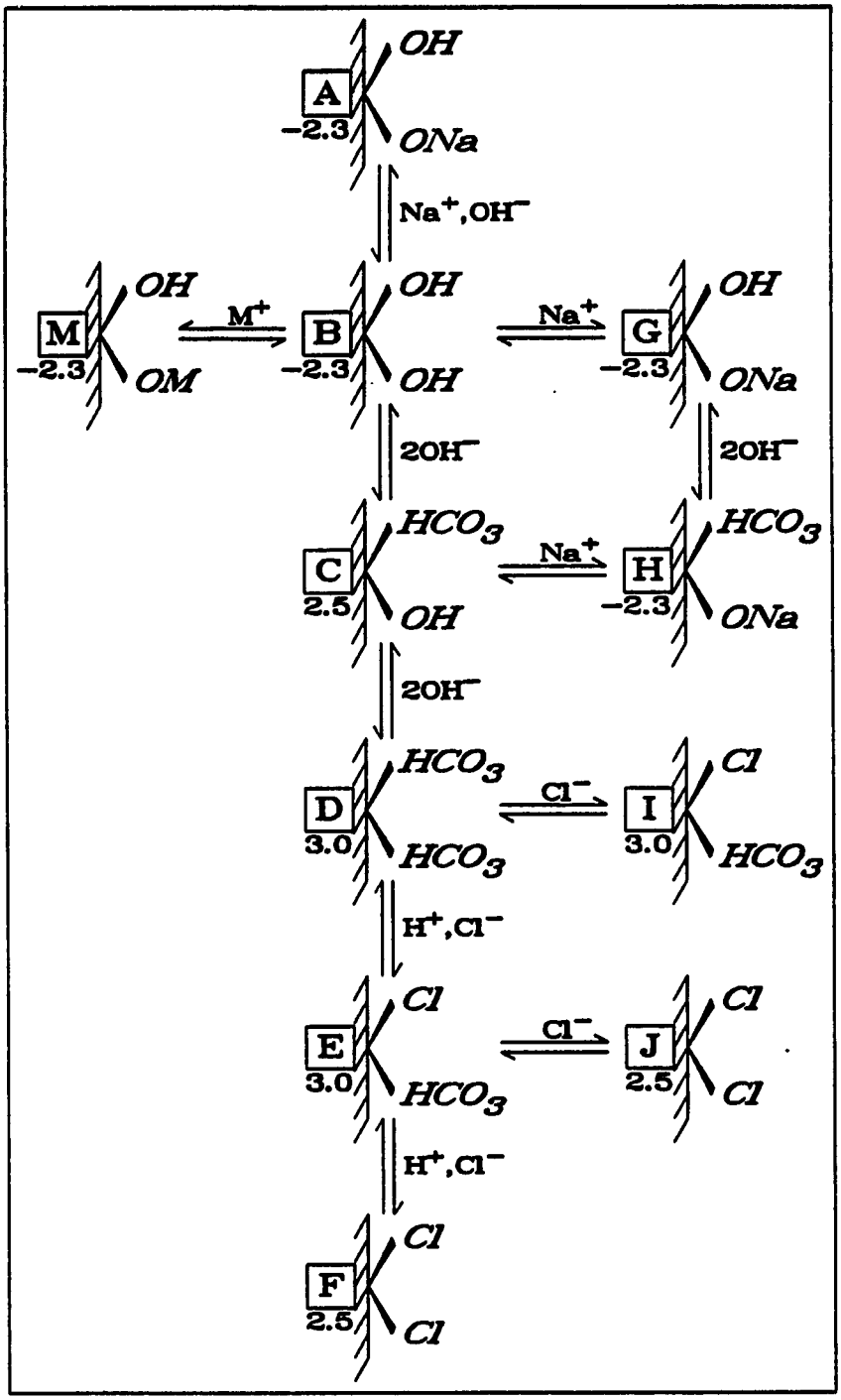

Fig. 4-2. Al oxide speciation model suggested in Chapter 3 with corresponding EM values. The EM values associated with each species is shown below their corresponding symbols; units are in μm cm V^{-1} s^{-1}.

The high surface charge values a few pH units above and below the ZPC using traditional potentiometric titration methods are generally not recognized as being unrealistic and inconsistent with electrokinetic data. To generate predictions for the σ_0–pH isotherm at least two parameters need to be determined: K^{int} values and the capacitance value if applying the constant capacitance model. The criteria for determining the magnitude of the assumed parameters is based on the goodness-of-fit of the generated predictions with the experimental data. The capacitance density cannot be determined experimentally and is often treated as an empirical, adjustable model parameter (Goldberg and Sposito, 1984). Since the traditional potentiometric titration data show a convex behavior at high and low pH values, the goodness-of-fit soon deteriorates. Multilayer models are more effective in predicting the titration data at higher σ_0 values. The entire procedure yields questionable conclusions, however, because the data are not true surface charge values when singular reference curve titration methods are used. The solubility behavior of the solid phase greatly overshadows the true surface adsorption reactions. The mathematical consequences of including the Boltzmann distribution term in Eq. [4.6] and [4.7] are, therefore, mostly tracking the solubility behavior of the solid phase.

[4.2.2] Electrophoretic Mobility Study

The Al oxide used for these experiments was the same washed oxide used in earlier potentiometric titration analyses (Chapter 3); i.e., γ-Al_2O_3 made by the Degussa Corp. of Teterboro, NJ, under the name of Aluminum Oxide C®. The oxide was believed to be clean of impurities, but may contain adsorbed CO_2 and a small amount of an unknown metal chloride (M^+Cl^-). The concentration of the stock Al oxide suspension was reported earlier to be 84.06 g L^{-1} and to have a specific surface area, using ethylene glycol monomethyl ether (EGME), of 83.1 m^2g^{-1}. The average primary particle size (dry) was 20 nm (supplied by the manufacturer).

Samples were prepared by adding 0.5 mL of the stock Al oxide suspension to 125-mL polyethylene bottles which were then pH adjusted with known quantities of either 0.24 *M* HCl or 0.24 *M* NaOH; the initial electrolyte concentration was adjusted with a concentrated NaCl solution. The total volume was kept constant at 70.0 mL with deionized water, and an N_2 atmosphere was maintained at all times. After equilibrating overnight on a reciprocating shaker, the pH of each suspension was measured and the electrophoretic mobility (EM) was analyzed on a Zeta-Meter (ZM-80) by Zeta-Meter, Inc., NY. The cell used was electrophoresis cell no. 1125 made by Zeta-Meter, Inc. The Plexiglas cell had the Pt electrodes separated by 10 cm. The manufacturer suggests that the conductivity be <0.1 S m^{-1} when

using Pt electrodes rather than Mo electrodes; otherwise $O_2(g)$ formation at the anode and $H_2(g)$ formation at the cathode will cause erroneous readings. The EM readings were obtained by measuring the time required for each particle to travel 160 μm under an applied potential (80–250 V) separated by 10 cm; that is, EM is the velocity of the particle (μm s^{-1}) induced by an applied electric field (cm V^{-1}), such that:

$$EM = \frac{160\mu m}{t} \times \frac{10cm}{V} \ , \ \left[\frac{\mu m \ cm}{V \ s}\right] . \qquad [4.9]$$

The EM was averaged over a maximum of 20 readings in two directions. The pH range studied was from 2.5 to 11.5, and the initial electrolyte concentrations were 0.0, 0.001, and 0.007 *M* NaCl. Several portions of the experiment were repeated to ensure reproducibility and detail of the resulting curves.

[4.3] RESULTS and DISCUSSION

The EM for the Al oxide with respect to pH, shown in Fig. 4-3, has two maximum values. At pH<7.0 the EM values are 3.0±0.5 μm cm V^{-1} s^{-1} with samples with low electrolyte concentrations having slightly higher EM values than samples with high electrolyte concentration. At pH>10.5 the EM values are –2.3 μm cm V^{-1} s^{-1} with no differences observed under various electrolyte concentrations. The zero point of charge (ZPC) decreased from 9.8 to 9.5 with increase in electrolyte concentration.

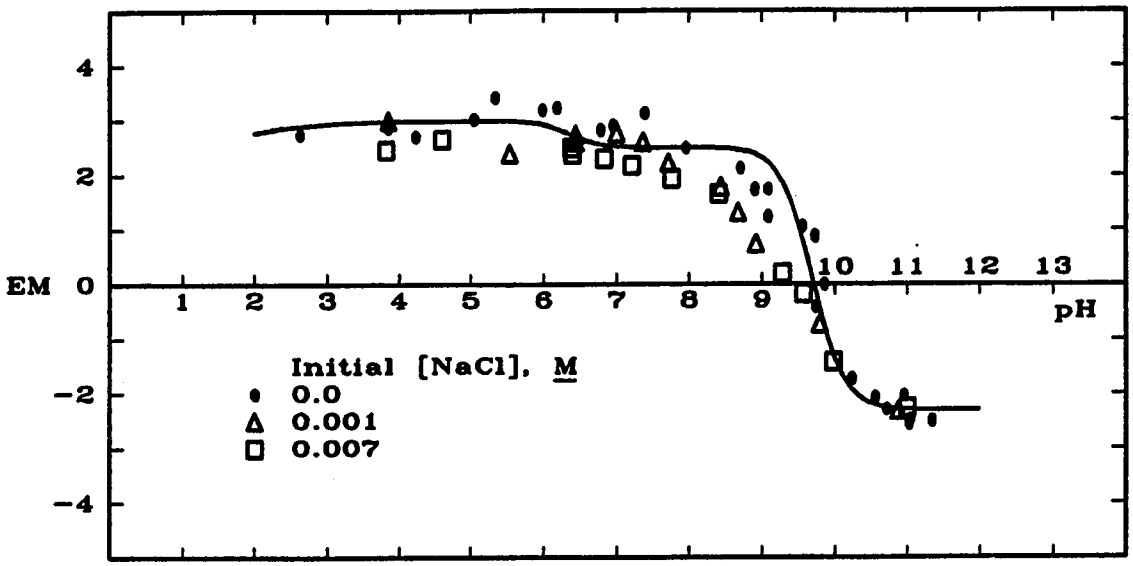

Fig. 4-3. Electrophoretic mobility vs. pH for Al oxide. Solid line is EM predicted based on speciation model illustrated in Fig. 4-2. Units are in μm cm V^{-1} s^{-1}.

The region between pH 7.0 and 10.5 is particularly interesting. The point of zero salt effect (PZSE) for this Al oxide was determined earlier in Chapter 3 to be at pH 7.5 for high electrolyte concentrations and at pH 7.76 for low electrolyte concentrations. Figure 4-3 does show a drop in the EM values at the above predicted PZSE values. The drop in the EM values are not sudden, but rather lower gradually from pH 7.5 to 9.5; at pH 9.5 to 10.5 the EM values do drop abruptly.

Suggestions for a physical interpretation of the surface reactions were outlined in Chapter 3 based on a potentiometric titration analysis modified by a backtitration step to adjust for the variable solubility of the solid phase. The model consists of pH and salt-dependent reactions, which are illustrated in Fig. 4-2 as the vertical reactions, and competitive salt-dependent (pH-independent) reactions, which are illustrated in Fig. 4-2 as the horizontal reactions. The key difference from other models is that there are no ions that are considered indifferent or inert, and the ion concentrations play an important role in the speciation of the surface. The model was mass balanced, and the equilibrium constants assumed that the surface ionization energy was constant. None of the values used was empirically adjusted; all the equilibrium values were directly derived from the data. Note that the physical description of the Al oxide surface as outlined in Fig. 4-2 is not confirmed; however, there is substantial evidence that the surface has adsorbed Cl^- at low pH and HCO_3^- or Na^+ at high pH conditions. These surface interpretations

do emphasize that ion adsorption on the surface does take place and that the oxide does not exist in a charged state in absence of a counterion. It is not possible to centrifuge the oxide suspension and use the packed oxide paste as either an anode or cathode.

This EM study shows that each type of surface species responds with varying degrees of mobility under an applied electric field. Predictions of the Al oxide's EM may be made based on mass balanced equations presented in Chapter 3. The EM values corresponding to each of the surface species shown in Fig. 4-2 were determined by matching the measured EM values with the surface species that was predicted dominant under the assigned conditions. The results show EM=2.5 (species C, F and J), 3.0 (species D, E and I), and -2.3 μm cm V^{-1} s^{-1} (species A, B, G, H, and M). That is, all the species that have cation adsorption (H^+, Na^+, M^+) yield a constant negative EM value; species having HCO_3^- or Cl^- adsorption yield a positive EM value. These EM values generate the line drawn in Fig. 4-3 for the condition of zero initial NaCl additions. The EM predictions for the samples with high electrolyte concentrations were slightly lower at pH <9.0; however, these predicted values still overestimated the experimental values. The suggested model predicts no sensitivity of EM values to salt concentrations at the extremely high and low pH values, but does predict some salt sensitivity for most pH conditions, particularly near the PZSE and ZPC. The prediction for the ZPC is excellent. From these observations and from the model outlined in Fig. 4-2, it follows that

the pH of ZPC lowers with increase in electrolyte concentration due to the increase in cation adsorption. Cation adsorption (or exchange for H^+ ions) also results in lower EM values in the pH region between the predicted PZSE and ZPC. This is in contradiction with the current view that cation adsorption increases EM values and anion adsorption decreases EM values (Parks, 1965; Singh and Uehara, 1986). This hypothesis, however, is consistent with the cation-anion adsorption data and potentiometric titration analyses discussed in Chapter 3.

These experiments indicate that the Boltzmann distribution of ions (Eq. [4.2]) may be misapplied in describing the oxide surface behavior. If a surface charge exists (as is illustrated by Eq. [4.4] and [4.5]), then a surface potential must also exist. However, if the surface is closely associated with counterions, or has no *net* surface charge (as is illustrated in Fig. 4-2), then Eq. [4.2] does not apply. The author suggests that the charge behavior observed by electrokinetics is a result of an electric field induced shearing of counterions from the surface (Fig. 4-4). More specifically, there is no net charge existing on the solid surface in absence of an applied electric field in water. Since the Al oxide does not exhibit a charged behavior when dry (Degussa Tech. Bull. 56), it follows that the shearing strength is a function of the dielectric constant of the medium and the bonding strength of the counterions onto the surface. Whereas traditional models treat the oxide as being capable of forming a true surface charge that induces ion adsorption, this model treats the oxide as being capable of undergoing ion exchange or substitution

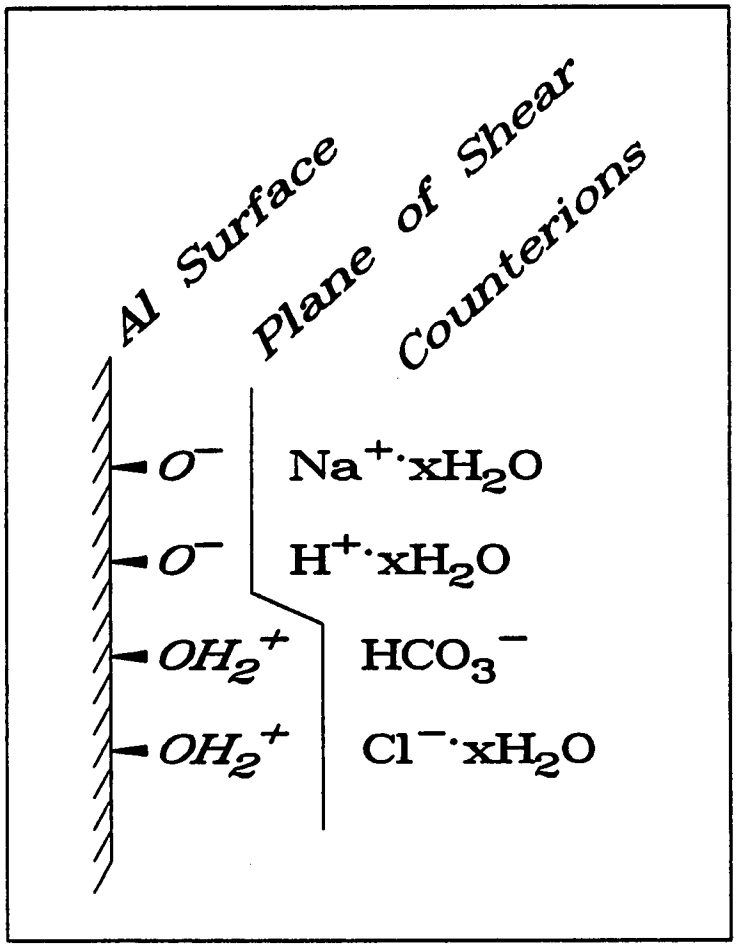

Fig. 4-4. Suggested location of plane of shear under an applied electric field.

reactions resulting in a surface that exhibits mobility in an applied electric field; the oxide surface remains neutral at all other times. The plane (or zone) of shear may be somewhere in a diffuse double-layer region (Hiemenz, 1977); however, the induced shearing is pictured here to be between the surface and the closely associated counterions (Fig. 4-4). This description is not affected if the counterions are hydrated, or if H_2O bridging exists between the counterions and the surface. Thus, the surface is always neutral, but will become temporarily charged if the counterions are sheared off by an applied electric field.

The author realizes that this hypothesis also needs to be tested in terms of explaining yet other phenomena observed in the solid-aqueous phase physical chemistry of oxides; including coagulation and other forms of electrokinetics. The research emphasis must be to pursue models that are consistent with data from a variety of independent experiments.

[4.4] CONCLUSIONS

The Al oxide studied exhibited positive mobility at low pH and negative mobility at high pH, with the ZPC at pH 9.5 to 9.8. The magnitude of the mobility was constant at the high pH values, but varied slightly with salt concentrations at the low pH values. The speciation model suggested in Chapter 3 can be used to model the EM behavior where each type of surface species (-Cl, -HCO_3, -OM) responds with varying degrees of mobility to an applied electric field. The

proposed model assumes that anion adsorption results in positive mobility, and cation adsorption results in negative mobility. The ZPC also lowers with increase in aqueous electrolyte concentration due to the increased cation adsorption.

There is no theoretical reason for cation-anion exchange methods, potentiometric titration methods, and electrokinetics to disagree with respect to describing the surface charge behavior. Chapter 3 demonstrated that the cation-anion exchange methods yield identical results to potentiometric methods if the solubility of the solid phase is accounted for. These EM studies also confirm the observations made by the former two methods.

The mathematical effect of the Boltzmann distribution term used in many surface charge models is most probably merely tracking the solubility behavior of the solid phase. There is no definitive proof for the theory of variable ionization energy. There is also no reason to ignore the solubility phenomena and thus allow the large "surface charge" values to remain unquestioned. Unless solubility phenomena are considered, the application of models that use the Boltzmann distribution term and singular reference potentiometric titration data, including the constant capacitance and diffuse double-layer (DDL) models, are questionable.

CHAPTER 5

CATION ADSORPTION STUDIES

on a

SILICON OXIDE

[5.1] INTRODUCTION

The maximum number of sites (Γ_{max}) that a solid phase can support is an essential parameter for modeling ion adsorption. The Γ_{max} values can be determined based on potentiometric titration data (Huang, 1981); however, the mathematical manipulation of the data can be rather difficult. The Langmuir (1918) equation has been used extensively in describing ion adsorption behavior, and the logical inclusion of a maximum adsorption limit makes it easy to use cation exchange capacity (CEC) and anion exchange capacity (AEC) data to estimate the Γ_{max} values. The dependence of these values on pH was described by Mattson (1931) and Kurbatov et al. (1951); subsequently, the CEC-AEC data is

measured under specific pH conditions (e.g., soil pH or pH 7.00). To ensure that the maximum CEC-AEC values are true Γ_{max} values, high ion concentrations are used as is predicted by the Langmuir equation. The highest ion adsorption values attainable are with high ion concentrations and at the extremely high or low pH values relative to the zero point of charge (ZPC).

For variable charge surfaces (e.g., oxides), traditional views state that CEC increases as pH increases because the solid phase (soil or colloid) has increased in negative charge. Similarly, AEC increases as pH decreases because the solid phase has increased in positive charge. Schematically, the surface charge reactions are

$$\text{surface-OH} \rightleftharpoons \text{surface-O}^- + \text{H}^+ \qquad [5.1]$$

$$\text{surface-OH}_2^+ \rightleftharpoons \text{surface-OH} + \text{H}^+ \qquad [5.2]$$

with surface–OH_2^+ existing at low pH values and adsorbing anions (high AEC), and surface–O^- existing at high pH values and adsorbing cations (high CEC). The adsorption phenomenon is predominantly an electrostatic attraction (non-specific adsorption). However, cation and anion adsorption are also known to displace H^+ cations and OH^- anions, respectively, from the surface. Thus, the concept of *exchange of bases* is extended to include the ions H^+ and OH^-. Schematically, the ion exchange (specific adsorption) reactions

$$\text{surface-OH} + \text{M}^+ \rightleftharpoons \text{surface-OM} + \text{H}^+ \qquad [5.3]$$

$$\text{surface-OH} + \text{L}^- \rightleftharpoons \text{surface-L} + \text{OH}^- \qquad [5.4]$$

modeled B adsorption envelopes by several Al oxides at various pH values and did not consider the possibility of Cl^- anion competition at low pH; their acidic pH adjustments were made with HCl. The Cl^- anion adsorption by Al surfaces is well documented (Hingston et al., 1972; see also Chapter 3).

Finally, the concepts of inert species as well as inner-sphere and outer-sphere complexes are introduced. The identification of inert species, or indifferent background electrolytes, is based on potentiometric titration data as described by Lyklema (1984). If the pH of ZPC, as measured with KNO_3 electrolyte, is shifted in the presence of another electrolyte, then the latter salt is considered specifically adsorbed. The KNO_3 electrolyte is assumed to be an ideal reference as an indifferent electrolyte. An electrostatic attraction to the species in Eq. [5.1] and [5.2] by an ion would be considered an outer-sphere complex provided that at least one solvent molecule (e.g., H_2O) is present between the surface and the adsorbing ion (Sposito, 1984). An inner-sphere complex would involve strong attractive forces and would be expected of ions that undergo exchange reactions as illustrated by Eq. [5.3] and [5.4]. The presence of ligand exchange is generally considered sufficient evidence of the existence of an inner-sphere complex (rather than outer-sphere). In situ spectroscopic analyses offer more direct evidence for differentiating the inner and outer-sphere surface complexes (Johnston and Sposito, 1987; Hayes et al., 1987). Inner and outer-sphere complexes have also been termed specific and non-specific adsorption (Hingston et al., 1967). If the

complex is inner-sphere, then the compounds involved should be included in mass action equations and rate laws (Stumm, 1986).

The exchange reactions outlined in Eq. [5.3] and [5.4] suggest that the changes in H^+ and OH^- concentrations should be stoichiometrically related to the changes in L^- anion and M^+ cation concentrations in the bulk solution. The H^+/cation stoichiometry, or ratio, is based on a comparison of potentiometric titration data with cation removal data. The potentiometric data offers, in theory, the amount of protons adsorbed or desorbed by the surface. Some values reviewed by Schindler (1981) and Kinniburgh and Jackson (1981) show a trend in the H^+/cation stoichiometric ratio with respect to pH; the ratio often increases with pH. Few OH^-/anion stoichiometry have been directly measured (Rajan, 1979; see also Chapter 3), but the methods are essentially the same as for the H^+/cation ratio determinations.

Current theories on pH effects on CEC and AEC were questioned in this dissertation (Chapters 2, 3, and 4). Earlier chapters have argued that the proton isotherms obtained by the traditional potentiometric titration methods are not accurate due to the variable solubility effects of the solid phase. It was also shown that all the background electrolytes are directly involved in the surface chemical reactions by cation and anion exchange (Eq. [5.3] and [5.4]), and that the surface charge reactions outlined by Eq. [5.1] and [5.2] are not correctly

describing the surface adsorption phenomenon. To assume that some ions are inert background electrolytes may easily result in errored conclusions. The concept of any true surface charge as observed from the bulk solution was challenged as well. That is, both the hydrated outer-sphere and dehydrated inner-sphere adsorbed ions are successful in maintaining a net neutral surface charge; both are also involved in mass action equations. The concept of competitive exchange reactions was hypothesized to be the only realistic approach towards surface adsorption modeling. Thus, L^- anion adsorption envelopes were described in terms of OH^- anion competition at high pH values, and Cl^- anion (or conjugate base to the acid used for the acidic pH adjustments) competition at low pH values. Furthermore, by correcting for the variable solubility effects by using a backtitration technique, the CEC-AEC data and the proton isotherm data both resulted in the same adsorption isotherm values. The Γ_{max} values were determined by direct observation of the data without any further mathematical manipulations.

In this chapter, the proton isotherm of a Si oxide was investigated using both NaCl and $MnCl_2$ electrolyte solutions and the backtitration technique (Chapter 2). The objectives were: (i) to characterize the proton isotherm behavior of a Si oxide, (ii) to study the pH effects on cation adsorption, and (iii) to correlate the cation adsorption isotherm with the proton isotherm. The Mn^{2+} cation was chosen for this study because it does not appreciably hydrolyze before precipitation occurs at pH near 8 (Baes and Mesmer, 1976).

[5.2] MATERIALS and METHODS

The colloid studied was SiO_2 made by J.M. Huber Corp. (Havre de Grace, MD) under the name Zeothix® 265. The manufacturer's specifications on this oxide are shown in Table 5-1. The manufacturing procedure for this Si oxide was described by Wason (1978).

The oxide was acid washed with HCl (pH = 3.22, conductivity = 0.26 S m^{-1}) followed by 8 H_2O washings to a final conductivity of 3860 μS m^{-1} (pH = 5.5). The H_2O used was purified through an ultrapure D8902 cartridge (Barnstead Co., Newton, MA) and N_2 purged for at least 15 min before each use. With each wash the sample was agitated overnight on a reciprocating shaker, and separated for 20 min on a RC-5B Sorvall centrifuge (DuPont Co., Wilmington, DE) at 11000–20000 $\times$ g. A N_2 atmosphere was maintained at all times, except during the removal of the oxide from the centrifuge tubes.

After the 8 H_2O washings, the sample was again resuspended in H_2O and used as the stock Si oxide suspension for all experiments. Approximately 1 L of stock solution was prepared and found to have a suspension concentration of 141.2 g L^{-1}. The objective of these washings was to obtain a Si oxide suspension that was free of unknown impurities, particularly CO_2 and Na_2SO_4.

Table 5-1: Huber Corp. specifications on Zeothix® 265.

SiO_2	89–92%
Al_2O_3	0–0.9%
Na_2O	0.5–1.0%
Na_2SO_4	maximum 1.5%
R_2O_3	0.04–0.12%
Loss on Ignition (1173 K)	3.5–5.5%
Density (298 K)	2.0 g mL^{-1}
Average Particle Size	1.5–2.0 μm
Surface Area (BET)	200–300 m^2g^{-1}

The adsorption behavior of H^+ ions on the Si oxide was determined by mass balance as outlined in the backtitration technique in Chapter 2. The procedure was modified by adding 5 mL of Si oxide suspension to 30 mL of pH/electrolyte concentration adjusted water. The pH was adjusted with known quantities of either 0.24 *M* HCl or 0.24 *M* NaOH; the electrolyte used was NaCl. Some samples had 1.000 mL of 1.75 *M* or 0.0175 *M* $MnCl_2$ solution added instead of the NaCl; thus, these samples had an initial $MnCl_2$ concentration of 0.053 *M* or 5.3×10^{-4} *M*. The total volume of each sample was 35 mL. The exclusion volume was estimated to be 0.353 mL. After equilibrating overnight, centrifuging and filtering through 0.2-μm GA-8 Gelman filter paper, the weighed supernatant was backtitrated with either 0.03 *M* NaOH or 0.03 *M* HCl. The end point pH varied from 4.7 to 8.0 depending on the Si solubility. The highly soluble alkaline suspensions (pH>8.8) had end points at pH$\leq$5.0. The low solubility concentrations under acidic conditions (pH<8) had end points at pH 8.0. The surface area was assumed to be 250 m^2g^{-1}.

Prior to backtitrating, some samples were analyzed for Mn^{2+} concentration remaining in solution with a Perkin Elmer 5000 Atomic Absorption spectrometer. These samples were diluted with 2% $CaCl_2$ solution to minimize Si interferences. Some samples were also analyzed for Cl^- concentration remaining in solution using an Orion Cl^- ion selective electrode. Several portions of each experiment were repeated to ensure reproducibility and detail of the resulting curves.

[5.3] RESULTS and DISCUSSION

The Mn^{2+} adsorption analysis, shown in Fig. 5-1 and 5-2, reconfirms the idea that cation adsorption occurs as a stoichiometric exchange reaction with surface cations, including the proton in surface–OH groups. For the samples with $5.3\times10^{-4}M$ $MnCl_2$, the shape of the adsorption isotherm (Fig. 5-1) is identical to the shape of the proton isotherm (Fig. 5-2), and each pH-independent region (or plateau) coincides exactly in both analyses. The arrows drawn through both Fig. 5-1 and 5-2 indicate the location of three plateaus. The line drawn through the adsorption isotherm data (Fig. 5-1) is merely highlighting the pattern observed; the solid line drawn through the proton isotherm data (Fig. 5-2) is the same line as the one drawn in Fig. 5-1 except it has been scaled down and mirror-inverted. Chapter 3 concluded that the stoichiometry of ion exchange with H^+ surface cations can only be observed if potentiometric backtitration methods are used; the data were exceptionally clear with the 1:1 stoichiometry of Cl^- ion exchange for OH^- surface anions on an Al oxide. These experiments further prove that when bulk solution pH is the variable, cation exchange or adsorption data should be consistent — and in agreement with — proton adsorption isotherms.

Plateaus of this nature have gone unnoticed by many researchers. A particularly significant study by James and Healy (1972) reported similar data with Co(II), Cr(II), and Fe(III) removal by a Si oxide. However, they did not

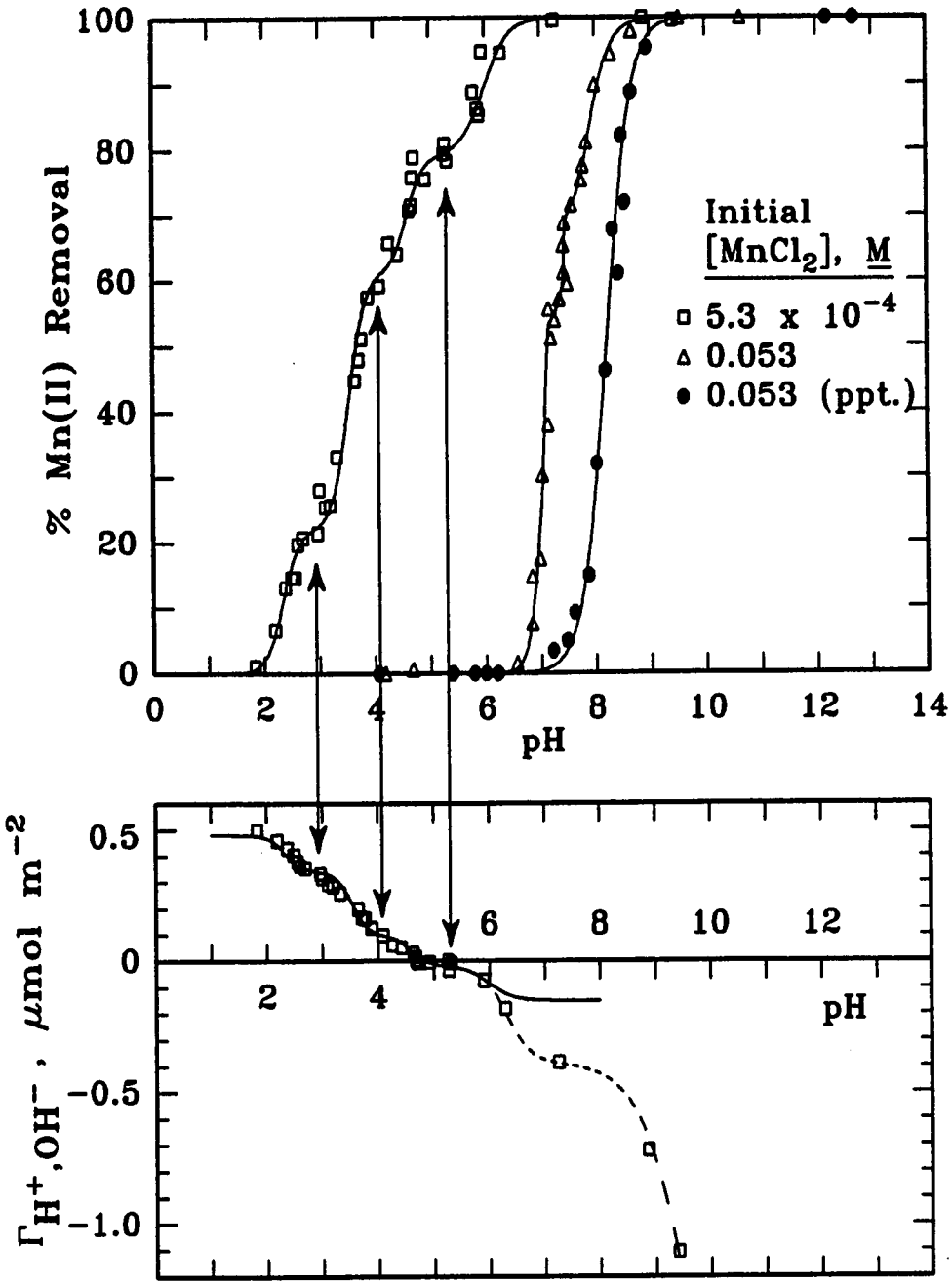

Fig. 5-1 (top). Percent Mn(II) removal vs. pH. Symbols (□) and (△) are with Si oxide present; (•) are precipitation analyses in the absence of Si oxide.

Fig. 5-2 (bottom). Backtitration analysis of Si oxide with $MnCl_2$. Initial $[MnCl_2]=5.3\times10^{-4}$ *M*. The arrows emphasize location of plateaus.

allude to the existence of plateaus even though their data showed plateaus nearly one pH unit wide for both Cr(III) and Co(II). Furthermore, their data could easily be sectioned into discrete pH-independent regions. Other examples of plateaus in cation removal vs. pH data include: NH_4^+ by a Chernozemic soil (Wada and Okamura, 1980), Na^+ by alkali soils (Gupta et al., 1985) and by kaolinite (Ferris and Jepson, 1975; Bolland et al., 1976), Pb^{2+} by Al oxide (Hohl and Stumm, 1976), and Cu^{2+} by an unspecified surface (Wang and Stumm *In* Stumm, 1986). These observations are not unique to cations; anion adsorption isotherms also display very clear plateaus.

In all the observations cited above, the recognition that a plateau is present seems to depend on its size. Small plateaus (even one pH unit wide) can be ignored without excessive error or deviation from model generated predictions. However, the transitions between these plateaus are fingerprint images of the pH-dependent surface/aqueous chemical reactions. To free-draw a smooth curve ignoring a series of plateaus (or steps) is most inappropriate. If such curves are model generated, then the model may be considered incomplete.

Another problem that is often observed involves presentation of a cation removal vs. pH isotherm with very few data points shown. To illustrate this, imagine the isotherm in Fig. 5-1 for low Mn^{2+} concentrations with only five or six data points. The researcher would probably have no hint of the existence of

these plateaus, and consequently draw a line covering five pH units connecting the data. It is easy to see how this may lead to further misinformation if the same researcher also performs experiments that are pH sensitive; e.g., rate of dissolution or adsorption experiments at an improperly selected fixed pH value. Note that at some pH values in Fig. 5-1, very small pH deviations result in large changes in the amount of cation removed; on the other hand, if the pH values are fixed at the location of the plateaus, then perhaps even moderate pH deviations may be tolerated without affecting the surface chemical characteristics.

Each plateau in Fig. 5-1 corresponds to a different surface chemistry; i.e., completion of one type of reaction, and initiation of another type of reaction. These are not due to an electrostatic sequence of reactions between a charged surface and the counterions in the bulk solution (Chapter 4). Instead, each sequence of the surface exchange reactions varies in its affinity for the H^+ or OH^- ions and, consequently, also varies in the pH values (or range) where H^+ buffering is observed.

The H^+/cation ratio determined from the data in Fig. 5-1 and 5-2 is 6.0 protons removed per Mn^{2+} adsorbed. It would be erroneous to conclude that each Mn^{2+} species occupies six surface sites. This observation may be explained by a number of complex reactions. An example of one such reaction is:

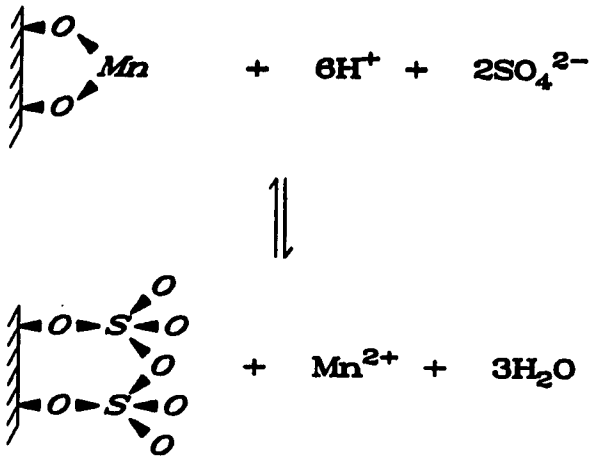

[5.5]

with formation of the pyrosulfate group ($S_2O_7^{2-}$) due to adsorption of neighboring sulfate groups (SO_4^{2-}), followed by an acid induced removal of one of the oxygens as H_2O. This reaction may be continuous with other neighboring SO_4^{2-} groups (see Nebergall et al., 1972; Purcell and Kotz, 1977). However, this cannot be pursued much further unless some spectroscopic evidence is also presented. On the other hand, given the information available in Table 5-1, this hypothesis may be used, at least tentatively, in surface adsorption modeling.

The proton isotherm of the Si oxide is shown in Fig. 5-3 at various initial NaCl concentrations. A significant observation is that there are three salt-dependent shifts at pH 8.5, 7.0, and <6.0. The latter salt-dependent shift is composed of several small transitions from pH 1.5 (and perhaps lower) to 6.0. This implies the existence of salt-dependent and competitive reactions similar to those hypothesized for Al oxide (Chapter 3).

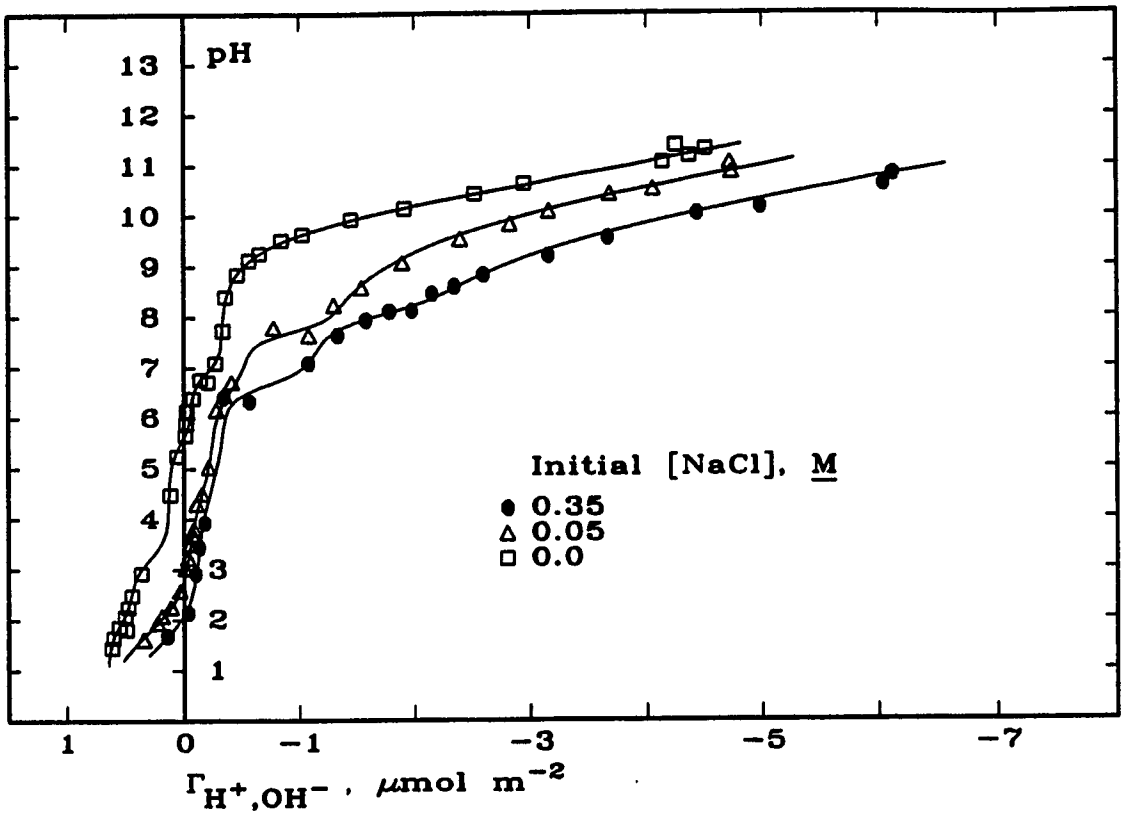

Fig. 5-3. Backtitration analysis of Si oxide at various ionic strengths.

Another significant observation is that there is no PZSE present; however, a PZSE may exist at very low pH values. No Cl^- removal was detected at any of the low pH values studied. Unfortunately, an analysis of SO_4^{2-} removal was not obtained. Parks (1965) reports an average zero point of charge (ZPC) at pH 2.0 for Si oxides based on electrokinetic data. Chapter 3 hypothesized that positive PZSE shifts on the proton isotherm data may be due to cation impurities present on the oxide prior to the titration analysis. Thus, this oxide may also have some cation impurities (e.g., surface–ONa groups) initially present in spite of the acid and H_2O washings. It is believed, however, that the isotherm observed in Fig. 5-3 is due predominantly to the Si surface. The major reported impurity is Al (Table 5-1), yet the proton isotherm shown does not exhibit any of the Al isotherm patterns studied earlier for Al oxide (Chapter 3). This is consistent with the data shown in Fig. 5-1 and 5-2; i.e., a Na-Mn exchange would show no H^+ release by the surface. At pH 5.0 (the average equilibrium pH without acid or base additions), Fig. 5-1 shows 78.1% Mn(II) removal, and Fig. 5-2 shows almost no H^+ removal.

The backtitration technique gives an accurate proton isotherm due to the correction for the pH-dependent solubility effects of the analysis. This is particularly important with Si oxide because of its extremely high solubility at the alkaline pH values; so much so, that nearly 1.0 mmol of NaOH is needed for the suspension to reach pH 10.5 (compared to 0.011 mmol for a blank). The excess NaOH added is consumed in forming aqueous species such as $SiO(OH)_3^-$,

The interpretation of these plateaus is merely tentative at this time. It is believed that the initiation of precipitation as $Mn(OH)_2(s)$ would result in increased (more pronounced) cation removal rather than the observed plateaus. Additionally, with increased cation removal by adsorption and lower cation concentration remaining in solution, the initiation of the precipitation reaction should be shifted to slightly higher pH values. A complication with this type of analysis is that Na^+ cation competition may be significant. At pH 7.3 and 7.6 the concentrations of Na^+ cations, introduced as NaOH alkaline pH adjustments, were 0.054 *M* and 0.071 *M*, respectively. Thus, these plateaus may be underestimating the Γ_{max} value.

[5.4] CONCLUSIONS

The proton isotherm behavior of the Si oxide showed pH and salt-dependent shifts. Modeling this Si oxide may involve competitive reactions similar to those discussed for Al oxide in Chapter 3; however, the available data are too incomplete to properly formulate a model at this time. The proton isotherm was relatively stable at pH<6 compared to the alkaline conditions.

A tentative attempt to determine the total number of sites present, based on Mn^{2+} adsorption data at high concentrations, resulted in 0.29 and 0.22 nm^2 $site^{-1}$ (equivalent to 0.87 and 0.66 nm^2 per surface Si if each Si is assumed to support three surface–OH groups).

The adsorption of cations resulted in easily identified pH regions or plateaus. These plateaus correlated extremely well with the proton isotherm analyses. It is strongly suggested that these plateaus be considered significant when illustrating cation (and anion) adsorption data. Surface adsorption models should at least be able to suggest the reactions involved to the left and right of each of the plateaus.

CHAPTER 6

SUMMARY and CONCLUSIONS

This dissertation is primarily concerned with the fate of cations and anions in terms of their adsorptive behavior onto oxide surfaces. The novelty of this research is a result of a new method for obtaining surface adsorption data of H^+ ions on oxide surfaces (Chapter 2); specifically, the variable solubility of the solid phase is considered as a significant source (or sink) for the H^+ ions. The assumption that various inert, or indifferent, ions exist in the bulk solution is questioned throughout this work. Whereas traditional studies treat pH, ionic strength, and adsorbing ions as three separable parameters, this research treats H^+ and OH^- ions as competitive cations and anions. That is, no ions are considered inert, and all ions and compounds possess varying degrees of affinity for the solid surface (Chapter 3). Generally, observations on the behavior of oxides have differed with the methods used, including: potentiometric titrations, ion

exchange, and electrokinetics. However, this dissertation argues that the various observations should agree if the methods are properly applied (Chapter 4). Finally, the emphasis is made on the importance of recognizing even small changes in ion adsorption patterns as significant indicators of surface chemical phenomena (Chapter 5). The following paragraphs give a more detailed description of each chapter.

In Chapter 2, batch potentiometric titration analyses were made on a γ-Al_2O_3 colloidal suspension and interpreted in terms of the electroneutrality principle. Three titration methods involving a singular reference curve were compared. The first reference used was theoretical, while the latter two were representative supernatant curves: an electrolyte solution, and an aliquot of the zero point of titration (ZPT) supernatant. All three methods resulted in similar charge isotherms and a zero point of charge (ZPC) = 8.60. A fourth titration method was developed involving each supernatant of the batch titration sample to act as a unique reference. This latter method is a backtitration technique which accounts for all sources that also consume H^+ ions, leaving the difference to be the adsorbed proton concentration only. The $NaClO_4$ electrolyte solution used is postulated to be adsorbed with competitive cation and anion exchange mechanisms with a point of zero salt effect (PZSE) = 7.50.

In Chapter 3, a backtitration technique was used to collect proton isotherm data for an Al oxide, and was found to be stoichiometrically related to the cation and anion isotherm behavior. The adsorption of various ions by the Al oxide surface was modeled based on: (i) two surface sites, (ii) pH+salt-dependent reactions (H^+ and Cl^-, $2OH^-$, or Na^+ and OH^-), (iii) competitive salt-dependent reactions (Na^+ or Cl^-), (iv) CO_2(aq) pH-dependent reactions with the surface–OH groups, and (v) presence of an unknown M^+Cl^- salt (0.0005 *M*). The total number of Al sites was 1.7 μmol m^{-2} or 3.4 μmol m^{-2} of total available sites. The pH of point of zero salt effect (PZSE) represented the surface condition in which the negative charges (or cation surfaces) equaled the positive charges (or anion surfaces); the cation exchange capacity (CEC) equaled the anion exchange capacity (AEC) at this value. The CEC–AEC data and proton isotherm data were stoichiometrically correlated. The pH of PZSE values ranged from 7.50 to 7.76 depending on the electrolyte concentration present, with lower values as the concentration increased. The negative shifts in the PZSE values are due to anion impurities initially present on the surface, and positive shifts are due to cation impurities.

In Chapter 4, the theory on variable ionization energy of surface sites was criticized based on inconsistencies of traditional potentiometric titration data (singular reference curve methods) with electrophoretic mobility (EM) data, and on the nature of dissolution of the solid phase. The mathematical consequences of

including the Boltzmann distribution term in models using intrinsic equilibrium constants are most probably merely to track the solubility behavior of the solid phase. The EM of an Al oxide was studied with respect to pH. The isotherm showed clear maximum mobility at low and high pH values with the zero point of charge (ZPC) ranging from pH 9.5 to 9.8. The ZPC lowers with increasing electrolyte concentration due to the increased competitive behavior of the cations in solution for the surface sites. Assuming a constant ionization energy of the surface sites, a mass balanced model that predicted both anion-cation adsorption data and potentiometric titration data (backtitration technique) also correlated well with the EM data. The EM behavior was modeled based on the varying mobility of each type of surface species present on the oxide at various pH values. Whereas traditional models treat the oxide as being capable of forming a surface charge that induces ion adsorption, this model treats the oxide as being capable of undergoing ion exchange or substitution reactions resulting in surfaces that exhibit mobility in an applied electric field. The proposed model assumes that anion adsorption results in positive mobility, and cation adsorption results in negative mobility.

In Chapter 5, cation adsorption data using $MnCl_2$ and the proton isotherm of a Si oxide were compared with pH as the variable. The cation adsorption data showed three distinct plateaus that correlated very well to plateaus observed in the proton isotherm analysis. These plateaus are very important to surface adsorption

modeling, and may be significant in determining experimental conditions for other soil and colloidal research. A H^+/Mn^{2+} ratio of 6.0 was also determined, and a tentative mechanism was suggested for this large value. The proton isotherm obtained using the backtitration technique has some pH and salt-dependent shifts that may involve competitive reaction mechanisms between the ions in solution and the oxide surface. In addition, cation adsorption studies were used to determine the total number of sites available. This resulted in 5.8 and 7.7 μmol m^{-2}. The author emphasizes that models describing the ion adsorption phenomena on solid surfaces may be oversimplified due to lack of a complete analysis of the experimental data.

REFERENCES and AUTHOR INDEX

Index page number appears in braces {} after each reference cited.

1. Arrhenius, O. 1922. Clay as an ampholyte. J. Am. Chem. Soc. 44:521–524. {3, 71}

2. Baes, C.F., and R.E. Mesmer. 1976. The hydrolysis of cations. John Wiley & Sons, Inc., New York. {95, 105}

3. Barrow, N.J. 1985. Reaction of anions and cations with variable-charge soils. Adv. Agron. 38:183–230. {36, 37}

4. Barrow, N.J., J.W. Bowden, A.M. Posner, and J.P. Quirk. 1980. An objective method for fitting models of ion adsorption on variable charge surfaces. Aust. J. Soil Res. 18:37–47. {27}

5. Bates, R.G. 1973. Determination of pH: Theory and practice. 2nd. ed. John Wiley & Sons, Inc., New York. {3}

6. Beyrouty, C.A., G.E. Van Scoyoc, and J.R. Feldkamp. 1984. Evidence supporting specific adsorption of boron on synthetic aluminum hydroxides. Soil Sci. Soc. Am. J. 48:284–287. {27}

7. Bloom, P.R., and M.S. Erich. 1987. Effect of solution composition on the rate and mechanism of gibbsite dissolution in acid solutions. Soil Sci. Soc. Am. J. 51:1131–1136. {92}

8. Bolland, M.D.A., A.M. Posner, and J.P. Quirk. 1976. Surface charge on kaolinites in aqueous suspension. Aust. J. Soil Res. 14:197–216. {101}

9. Böttger, W. 1897. Die Anwendung des Elektrometers als Indikator beim Titrieren von Säuren und Basen. Zeitschrift für Physikalische Chemie (Leipzig). 24:253–301. {3}

10. Bowden, J.W., A.M. Posner, and J.P. Quirk. 1977. Ionic adsorption on variable charge mineral surfaces. Theoretical-charge development and titration curves. Aust. J. Soil Res. 15:121–136. {10}

11. Bradfield, R. 1923. The nature of the acidity of the colloidal clay of acid soils. J. Am. Chem. Soc. 45:2669–2678. {8, 71}

12. Bradfield, R. 1924. The effect of the concentration of colloidal clay upon its hydrogen ion concentration. J. Phys. Chem. 28:170–175. {8}

13. Brunauer, S.L., P.H. Emmett, and E. Teller. 1938. Adsorption of gases in multimolecular layers. J. Am. Chem. Soc. 60:309–319. {14, 40, 97}

14. Chalmers, T.W. 1949. Historic researchers, chapters in the history of physical and chemical discovery. Morgan Brothers Ltd., London. {2}

15. Chapman, D.L. 1913. A contribution to the theory of electrocapillarity. Philosophical Mag. and J. of Sci. (series 6) 25:475–481. {3. 12}

16. Dayhuff, W.C., and D.R. Hoagland. 1924. The electrical charge on a clay colloid as influenced by hydrogen-ion concentration and by different salts. Soil Sci. 18:401–408. {71}

17. Degussa Corp. 1984. Technical Bulletin Pigments no. 56. 4th ed. Degussa Corp., Teterboro, NJ. {86}

18. Ferris, A.P., and W.B. Jepson. 1975. The exchange capacities of kaolinite and the preparation of homoionic clays. J. Colloid Interface Sci. 51:245–259. {31, 101}

19. Figurovsky, N. 1973. Johann Tobias Lovits (Lowitz). p. 519–520. *In* C.C. Gillispie (ed.) Dictionary of Scientific Biography. Vol. 8. Charles Scribner's Sons, New York. {2, 34}

20. Fisher, E.A. 1921a. Studies on soil reaction. I. A résumé. J. Agric. Sci. 11:19–44. {3}

21. Fisher, E.A. 1921b. Studies on soil reaction. II. The colorimetric determination of the hydrogen ion concentration in soils and aqueous soil extracts. J. Agric. Sci. 11:45–65. {3}

22. Goldberg, S. 1985. Chemical modeling of anion competition on goethite using the constant capacitance model. Soil Sci. Soc. Am. J. 49:851–856. {92}

23. Goldberg, S., and R.A. Glaubig. 1985. Boron adsorption on aluminum and iron oxide minerals. Soil Sci. Soc. Am. J. 49:1374–1379. {92}

24. Goldberg, S., and G. Sposito. 1984. A chemical model of phosphate adsorption by soils: I. Reference oxide minerals. Soil Sci. Soc. Am. J. 48:772–778. {74, 80}

25. Gouy, G. 1910. Sur la constitution de la charge électrique à la surface d'un électrolyte. J. Phys. Radium (série 4) 9:457–468. {3, 12}

26. Grahame, D.C. 1947. The electrical double layer and the theory of electrocapillarity. Chem. Rev. 41:441–501. {9}

27. Gupta, R.K., D.K. Bhumbla, and I.P. Abrol. 1985. Release of exchangeable sodium from an alkali soil upon amendment application — role of variable charge and exchangeable cation hydrolysis. Soil Sci. 139:312–318. {101}

28. Hayes, K.F., A.L. Roe, G.E. Brown, Jr., K.O. Hodgson, J.O. Leckie, and G.A. Parks. 1987. In situ x-ray absorption study of surface complexes: Selenium oxyanions on α-FeOOH. Science 238:783–786. {5, 93}

29. Heilman, M.D., D.L. Carter, and C.L. Gonzalez. 1965. The eyhylene glycol monoethyl ether (EGME) technique for determining soil surface area. Soil Sci. 100:409–413. {39}

30. Helmholtz, H. 1879. Studien über electrische Grenzschichten. Ann. Physik u. Chemie (Leipzig) 7:337–382. {3}

31. Hendershot, W.H. 1978. Measurement technique effects of the value of zero point of charge and its displacement from zero point of titration. Can. J. Soil Sci. 58:439–442. {10}

32. Hendershot, W.H., and L.M. Lavkulich. 1979. The effect of sodium chloride saturation and organic matter removal on the value of zero point of charge. Soil Sci. 128:136–141. {27}

33. Hiemenz, P.C. 1977. Principles of colloid and surface chemistry. Marcel Dekker, Inc., New York. {74, 88}

34. Hingston, F.J., R.J. Atkinson, A.M. Posner, and J.P. Quirk. 1967. Specific adsorption of anions. Nature (London) 215:1459–1461. {67, 93}

35. Hingston, F.J., A.M. Posner, and J.P. Quirk. 1972. Anion adsorption by goethite and gibbsite. I. The role of the proton in determining adsorption envelopes. J. Soil Sci. 23:177–192. {67, 93}

36. Hohl, H., and W. Stumm. 1976. Interaction of Pb^{2+} with hydrous γ-Al_2O_3. J. Colloid Interface Sci. 55:281–288. {29, 101}

37. Huang, C.P. 1981. The surface acidity of hydrous solids. p. 183–217. *In* M.A. Anderson and A.J. Rubin (ed.) Adsorption of inorganics at solid-liquid interfaces. Ann Arbor Science Publ., Ann Arbor, MI. {25, 36, 58, 73, 90}

38. Huang, C.P., and W. Stumm. 1973. Specific adsorption of cations on hydrous γ-Al_2O_3. J. Colloid Interface Sci. 43:409–420. {27, 36}

39. Ihde, A.J. 1984. The development of modern chemistry. Dover Publ., Inc. New York. {1}

40. James, R.O., and T.W. Healy. 1972. Adsorption of hydrolyzable metal ions at the oxide-water interface. I. Co(II) adsorption on SiO_2 and TiO_2 as model systems. J. Colloid Interface Sci. 40:42–52. {99}

41. Johnson, S.W. 1859. On some points of agricultural science. Am. J. Sci. Arts (series 2) 28:71–85. {2}

42. Johnston, C.T., and G. Sposito. 1987. Disorder and early sorrow: Progress in the chemical speciation of soil surfaces. p. 89–99. *In* L.L. Boersma (ed.) Future developments in soil science research. Soil Sci. Soc. Am., Inc., Madison, WI. {93}

43. Kayser, H. 1881. Ueber die Verdichtung von Gasen an Oberflachen in ihrer Abhängigkeit von Druck und Temperatur. Annalen der Physik und Chemie (Leipzig) 12:526–537. {2}

44. Kinniburgh, D.G., and M.L. Jackson. 1981. Cation adsorption by hydrous metal oxides and clay. p. 91–160. *In* M.A. Anderson and A.J. Rubin (ed.) Adsorption of inorganics at solid-liquid interfaces. Ann Arbor Science, Ann Arbor, MI. {94}

45. Kurbatov, M.H., G.B. Wood, and J.D. Kurbatov. 1951. Isothermal adsorption of cobalt from dilute solutions. J. Phys. Colloid Chem. 55:1170–1182. {4, 90}

46. Langmuir, I. 1918. The adsorption of gases on plane surfaces of glass, mica and platinum. J. Am. Chem. Soc. 40:1361–1403. {35, 90}

47. Lyklema, J. 1968. The structure of the electrical double layer on porous surfaces. J. Electroanal. Chem. Interfacial Electrochem. 18:341–348. {10, 28, 36, 72}

48. Lyklema, J. 1984. Points of zero charge in the presence of specific adsorption. J. Colloid Interface Sci. 99:109–117. {93}

49. Martin, R.R., and R.St.C. Smart. 1987. X-ray photoelectron studies of anion adsorption on goethite. Soil Sci. Soc. Am. J. 51:54–56. {42, 92}

50. Mattson, S. 1926. The relation between the electrokinetic behavior and the base exchange capacity of soil colloids. J. Am. Soc. Agron. 18:458–470. {71}

51. Mattson, S. 1931. The laws of soil colloidal behavior: VI. Amphoteric behavior. Soil Sci. 32:343–365. {3, 4, 9, 90}

52. McBain, J.W. 1909. The mechanism of the adsorption ("sorption") of hydrogen by carbon. Phil. Mag. (series 6, vol. 18) 108:916–935. {2}

53. Nebergall, W.H., F.C. Schmidt, and H.F. Holtzclaw, Jr. 1972. General chemistry. 4th ed. D.C. Heath and Co., Lexington, MA. {103}

54. Nernst, W. 1889. Die elektromotorische Wirksamkeit der Jonen. Zeitschrift für Physikalische Chemie (Leipzig) 4:129–181. {13}

55. Nordenskiöld, A.E. 1892. p. 61. *Quoted In* G. Urdang. 1942. The apothecary chemist, Carl Wilhelm Scheele. Am. Institute of the History of Pharmacy, Madison, WI. {2}

56. Olsen, S.R., and F.S. Watanabe. 1957. A method to determine a phosphorus adsorption maximum of soils as measured by the Langmuir isotherm. Soil Sci. Soc. Am. Proc. 21:144–149 {36}

57. Parfitt, R.L. 1980. Chemical properties of variable charge soils. p. 167–194. *In* B.K.G. Theng (ed.) Soils with variable charge. N.Z. Soc. of Soil Sci., Lower Hutt, New Zealand. {10}

58. Parker, J.C., L.W. Zelazny, S. Sampath, and W.G. Harris. 1979. A critical evaluation of the extension of zero point of charge (ZPC) theory to soil systems. Soil Sci. Soc. Am. J. 43:668–674. {10, 28, 76}

59. Parks, G.A. 1965. The isoelectric points of solid oxides, solid hydroxides, and aqueous hydroxo complex systems. Chem. Rev. 65:177–198. {10, 42, 86, 105}

60. Parks, G.A. 1967. Aqueous surface chemistry of oxides and complex oxide minerals. Isoelectric point and zero point of charge. Adv. Chem. Ser. 67:121–160. {10}

61. Parks, G.A., and P.L. de Bruyn. 1962. The zero point of charge of oxides. J. Phys. Chem. 66:967–973. {10, 27, 76}

62. Perrott, K.W., B.F.L. Smith, and R.H.E. Inkson. 1976. The reaction of fluoride with soils and soil minerals. J. Soil Sci. 27:58–67. {31}

63. Purcell, K.F., and J.C. Kotz. 1977. Inorganic chemistry. W.B. Saunders Co., Philadelphia. {103}

64. Rajan, S.S.S. 1979. Adsorption of selenite, phosphate and sulphate on hydrous alumina. J. Soil Sci. 30:709–718. {94}

65. Romm, E.S., and A.A. Rubashkin. 1985. Theory of the electric double layer on an oxide-electrolyte-solution boundary. Colloid J. USSR 47:463–470. (Engl. Transl.) Kolloidnyi Zhurnal 47:545–552. {36}

66. Schindler, P.W. 1981. Surface complexes at oxide-water interfaces. p. 1–49. *In* M.A. Anderson and A.J. Rubin (ed.) Adsorption of inorganics at solid-liquid interfaces. Ann Arbor Science, Ann Arbor, MI. {94}

67. Schindler, P.W., and H. Gamsjäger. 1972. Acid-base reactions of the TiO_2 (anatase)-water interface and the point of zero charge of TiO_2 suspensions. Kolloid Z.u.Z. Polymere 250:759–763. {70}

68. Schofield, R.K. 1949. Effect of pH on electric charges carried by clay particles. J. Soil Sci. 1:1–8. {9, 72}

69. Singh, U., and G. Uehara. 1986. Electrochemistry of the double layer: principles and applications to soils. p. 1–38. *In* D.L. Sparks (ed.) Soil physical chemistry. CRC Press, Inc., Boca Raton, FL. {86}

70. Sørensen, S.P.L. 1909. Enzymstudien. II. Mitteilung. Über die Messung und die Bedeutung der Wasserstoffionen konzentration bei enzymatischen Prozessen. Biochemische Zeitschrift 21:131–200,201–304. {3}

71. Sposito, G. 1981. The operational definition of the zero point of charge in soils. Soil Sci. Soc. Am. J. 45:292–297. {10}

72. Sposito, G. 1983. On the surface complexation model of the oxide-aqueous solution interface. J. Colloid Interface Sci. 91:329–340. {37}

73. Sposito, G. 1984. The surface chemistry of soils. Oxford University Press, New York. {37, 65, 72, 93}

74. Stumm, W. 1986. Coordinative interactions between soil solids and water — an aquatic chemist's point of view. Geoderma 38:19–30. {94, 101}

75. Stumm, W., and J.J. Morgan. 1981. Aquatic chemistry. 2nd. ed. John Wiley & Sons, Inc., New York. {28, 43, 51, 75}

76. Syers, J.K., M.G. Browman, G.W. Smillie, and R.B. Corey. 1973. Phosphate sorption by soils evaluated by the Langmuir adsorption equation. Soil Sci. Soc. Am. Proc. 37:358–363. {92}

77. Thomas, G.W. 1977. Historical developments in soil chemistry: Ion exchange. Soil Sci. Soc. Am. J. 41:230–238. {2}

78. Thompson, H.S. 1850. On the absorbent power of soils. J. Royal Agric. Soc. Engl. 11:68–74. {2}

79. Urdang, G. 1942. The apothecary chemist, Carl Wilhelm Scheele. Am. Institute of the History of Pharmacy, Madison, WI. {2}

80. van Riemsdijk, W.H., J.C.M. de Wit, L.K. Koopal, and G.H. Bolt. 1987. Metal ion adsorption on heterogeneous surfaces: Adsorption models. J. Colloid Interface Sci. 116:511–522. {78}

81. Veitch, F.P. 1904. Comparison of methods for the estimation of soil acidity. J. Am. Chem. Soc. 26:637–662. {8}

82. Wada, K., and Y. Okamura. 1980. Electric charge characteristics of ando A_1 and buried A_1 horizon soils. J. Soil Sci. 31:307–314. {101}

83. Wason, S.K. 1978. Cosmetic properties and structure of fine-particle synthetic precipitated silicas. J. Soc. Cosmet. Chem. 29:497–521. {96}

84. Way, J.T. 1850. On the power of soils to absorb manure. J. Royal Agric. Soc. Engl. 11:313–379. {2}

85. Way, J.T. 1852. On the power of soils to absorb manure. J. Royal Agric. Soc. Engl. 13:123–143. {2}

86. Westall, J., and H. Hohl. 1980. A comparison of electrostatic models for the oxide/solution interface. Adv. Colloid Interface Sci. 12:265–294. {9, 37, 74}

87. Yopps, J.A., and D.W. Fuerstenau. 1964. The zero point of charge of alpha-aluminum. J. Colloid Sci. 19:61–71. {13}